LUT UNIVERSITY
LUT School of Energy Systems
LUT Mechanical Engineering

Rudolf Silander

DESIGN CONSIDERATIONS FOR ADDITIVELY MANUFACTURED PARTS ON A SURFACE MISSION TO ENCELADUS

Examiners: Docent Heidi Piili
Professor Antti Salminen

Advisor: MSc. Leo Nyman

TIIVISTELMÄ

LUT-Yliopisto
LUT School of Energy Systems
LUT Kone

Rudolf Silander

Lisäävän valmistuksen suunnittelussa huomioitavia asioita: Case Enceladuksen pinnalle tehtävä avaruusmissio

Diplomityö

2019

79 sivua, 43 kuvaa, 15 taulukkoa ja 1 liite

Tarkastajat: Dosentti Heidi Piili TkT
Professori Antti Salminen TkT

Ohjaaja: Leo Nyman DI

Hakusanat: Lisäävä valmistus, 3D-tulostus, avaruus, planeettojen suojelu, kontaminaation hallinta, Enceladus, polymeerit

Tämän tutkimuksen tavoitteena oli tutkia lisäävän valmistuksen suunnittelussa huomioitavia asioita, kun kohteena on Enceladuksen (Saturnuksen kuu) pinta. Kirjallisessa osiossa koottiin tietoa tutkimuksista, joissa on käytetty lisäävää valmistusta avaruussovelluksissa sekä kartoitettiin materiaalivaatimuksia avaruussovelluksiin. Kokeellisessa osiossa tutkittiin avaruusalan standardin mukaista kontaminaation vähennysmenetelmää ja sen vaikutuksia lisäävästi valmistettuihin koekappaleihin.

Kirjallisuusosan päätuloksia oli, että polymeerien käyttö avaruudessa on rajoitettua johtuen kaasuuntumisilmiöstä tyhjiössä. Toisena tuloksena selvisi ajan ja lämpötilan vaikutus kokonaiskontaminaatiotasoon, suoritettaessa kontaminaatiovähennys kuivalämpö-menetelmällä. Polymeerien käyttöä avaruudessa todettiin rajoittavan standardien mukaiset vaatimukset kaasuuntumisesta, jolloin on tiedettävä materiaalin kokonaishaihtuma tyhjiön vaikutuksesta. Valitun kuivalämpömenetelmän lämpötila ja altistusaika riippuu halutusta kontaminaationvähennyksen tasosta.

Kokeellisessa osiossa nähtiin, että lämpö oli kutistanut koekappaleiden kokonaispituutta, mutta ei vaikuttanut vetolujuuksiin verrattuna käsittelemättömiin koekappaleisiin.

Kappaleiden muut mitat pysyivät muuttumattomina. Erot vetolujuuksissa käsiteltyjen ja käsittelemättömien koekappaleiden välillä todettiin olevan noin 0.2 MPa.

ABSTRACT

LUT University
LUT School of Energy Systems
LUT Mechanical Engineering

Rudolf Silander

Design considerations for additively manufactured parts on a surface mission to Enceladus

Master's thesis

2019

79 pages, 43 figures, 15 tables and 1 appendix

Examiners: Docent Heidi Piili, D. Sc. (Tech.)
Professor Antti Salminen, D.Sc. (Tech.)

Advisor: Leo Nyman, M.Sc (Tech)

Keywords: Additive manufacturing, 3D-printing, space, planetary protection, bioburden control, Enceladus, polymers

This thesis aimed to study design considerations for additively manufactured parts on a specific mission profile to the surface of Enceladus (moon of Saturn). The literature review gathered information on additive manufacturing use cases in space and material requirements in space. The experimental part presents a novel real-life example of implementing a bioburden reduction method on the additively manufactured test specimen and observing the effects of the process.

The main results from the literature review are the limitations in utilizing polymers in the vacuum of space due to the outgassing and effects of process parameters on bioburden utilizing a standard bioburden reduction method. Industry standards limit polymers with outgassing rates. The reduction magnitude of the dry heat method applied depends on the temperature and time.

The tests carried out in the experimental part of this thesis showed the effects of the elevated temperature, which resulted in the part shrinking, but did not affect the tensile strength when compared to untreated specimens. The specimens held dimensions in other directions. The difference in tensile strength was numerically confirmed to be approximately less than 0.2 MPa between treated and untreated specimens.

ACKNOWLEDGEMENTS

The completion of this thesis would not have been possible without the help of academic professionals from LUT and Aalto universities. Throughout the writing of this thesis, constructive guidance was received, which assisted in moving forward when challenges were faced.

In order to cope with daily struggles during the writing of this thesis, positive thoughts were kept up by my beloved spouse and family.

A humble thank you to you all.

Rudolf Silander
Vantaa 9.12.2019

TABLE OF CONTENTS

LIST OF SYMBOLS AND ABBREVIATIONS

3D	3-dimensional
AU	Astronomical Unit
D(hours)	Dry-heat process time [h]
T	Process temperature [ºC]
Tg	Glass transition temperature [ºC]
AM	Additive Manufacturing
ASTM	American Society for Testing and Materials
CAD	Computer-Aided Design
COSPAR	Committee on Space Research
COTS	Components Off The Shelf
DfAM	Design for Additive Manufacturing
DfMA	Design for Manufacture and Assembly
DH	Dry Heat, a bioburden control process
ESA	European Space Agency
FDM	Fused Deposition Modeling
FFF	Fused Filament Fabrication
INTA	Spanish National Aerospace Institute
ISO	International Organization for Standardization
MarCO	Mars Cube One
ME	Material Extrusion
NASA	National Aeronautics and Space Administration
PP	Planetary Protection
SAL	Sterility Assurance Level
VHP	Vapor Hydrogen Peroxide, a bioburden control process

1 INTRODUCTION

Exploring the unknown, a never-ending part of human nature embedded in each one of us. In the last century, humankind has made significant leaps forward in exploring the worlds beyond our home planet Earth. While centuries-old astronomy has been able to determine fundamental laws and make first scientific astronomical studies, recent strides have been enablers of both in-situ and in-space discoveries (Halliday *et al.*, 2011). Current space missions have provided a wide range of scientific data, ranging from planets to sample return missions from asteroids. One of these sample-return missions was the Japanese led Hayabusa 2 initially launched in 2014 and later in 2019 arrived at a near-Earth asteroid named Ryugu. As with most space missions, a consortium of partners from space agencies to industrial have together enabled the success of the mission, highlighting the importance of co-operation (Watanabe *et al.*, 2017).

Seeing the abundance of life around us on Earth, one might think it is self-explanatory that it might be found on planetary bodies all around the Universe. On the other hand, it is hard to imagine what indigenous life forms would present themselves, let alone how to accurately detect them. In addition to these already challenging conditions, there is a risk of unintentionally transferring life forms from our home planet to the planetary body at hand. In this form of scientific exploration, in which signs of life are searched for, an important concept called Planetary Protection (PP) emerges. The Committee on Space Research (COSPAR) has set forth a PP policy document to be complied with across the global scientific community (Meltzer, 2011, p. 13).

Since the dawn of the space age in the mid-20th-century, PP has been a topic of discussion amongst scientists all around. While it has been widely used to ensure future scientific discoveries, it continues to receive criticism on some regions of protection. Especially the search for life on Mars has been claimed to be in the border of overprotection, possibly slowing down the rate of discovery on this neighboring planet. It was claimed that exist a couple of issues when exploring life. Some previous spacecraft missions, especially to Mars, have been poorly cleaned. This has led to minor contamination already. Possible false positive readings from contaminants may as likely have originated from a planetary exchange of materials over the planet's history. A slowing factor for the new generation of spacecraft relates to the difficulty of applying cleaning measures, bioburden control, on the recently developed Cube Satellites (CubeSat) (Fairén *et al.*, 2019). Figure 1 presents the standardized satellite platform, known as CubeSat.

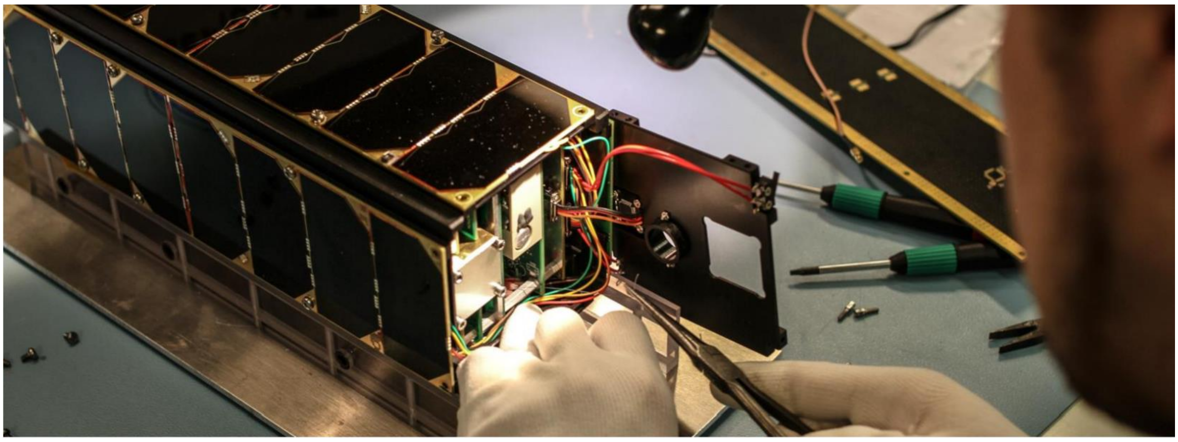

Figure 1. The first Finnish satellite Aalto-1, a CubeSat developed by the Aalto University (Praks *et al.*, 2015).

In recent years, the CubeSat standard has been adopted by a large variety of both industrial space companies, start-ups, as well as universities teaching essential skills for space-related projects. The document has been prepared by California Polytechnic, San Louis Obispo, and Stanford University and made publicly available to anyone (Mladenić *et al.*, 2014, p. 5). One of the pioneering universities in Finland in the field of CubeSats has been Aalto University based in Espoo, Finland.

Further iterations of the initially launched Aalto-1 have been developed in co-operation with university students and mentors alike. For the author, it was a pleasure to be a part of the currently developed Aalto-3 CubeSat, still under development and manufacturing. It truly gave a solid understanding of space project management and taught valuable lessons on technological requirements and the importance of communication.

Previously, the CubeSat generation has been launching off Earth to near-Earth orbits, such as the commonly utilized low-Earth-orbit (LEO). As part of the design philosophy behind most CubeSats is taking advantage of the readily available COTS-components (Commercial of the Shelf), which has enabled reasonable cost structures for university projects and other industrial players (Lyke, 2012). Currently, interplanetary missions have been pursued and planned, with the way paved by the first interplanetary CubeSats Mars Cube One (MarCO), one and two, launched in 2018. With the nearest flyby of Mars occurring in late 2018, it indeed marked the era of interplanetary CubeSat exploration (Klesh and Krajewski, 2018). Recent developments and a change of mindset from a traditional space agency led exploration effort to an extensively spread effort, has been driving humankind's understanding of the universe forward. The importance of large-scale missions managed by agencies should not be underestimated. Traditional know-how acquired from the decades of technological development and standardization might be thought to have built up the capability enough to enable the maturity levels required to develop such CubeSat missions.

When it comes to supporting any of these complex space missions, state-of-the-art manufacturing methods are required to achieve the scientific goals driving the missions. One of these methods is called additive manufacturing (AM), and in short terms, it is contrary to traditional subtractive manufacturing (SM). Some commonly utilized SM methods include milling, turning, and grinding. All these methods work to remove material from the first piece of raw material to form the final end-piece. It is possible to create complex shapes with AM by forming the raw material, layer-by-layer, close to the final end-piece. One of the main advantages of AM is that only the material which is required is used in manufacturing (Gibson *et al.*, 2010, p. 7, p. 34). Figure 2 shows a commercially available AM method, referred to as material extrusion (ME), where a nozzle is dispensing the raw material.

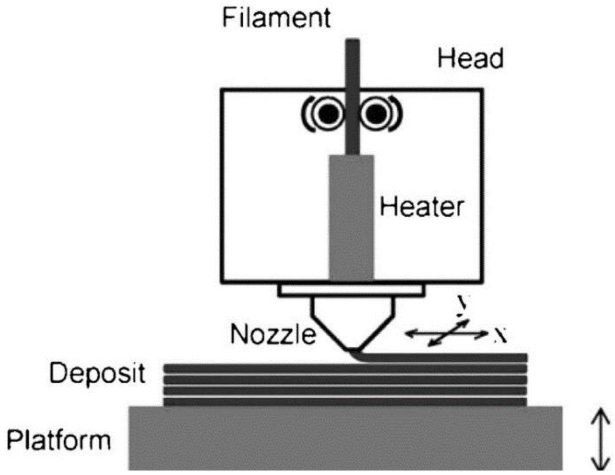

Figure 2. Filament dispensing ME machine for layer-by-layer manufacturing (Singh et al., 2018).

The technological developments between 1950s and 1980s lead to the first AM machines being realized in mid-1980s. One of the pioneers, in the field of AM machines, was Charles Hull, who later founded the 3D Systems company, which is still operational in 2019 (Gibson *et al*., 2010, p. 7, p. 34). A photograph of the first machine developed by Charles Hull is presented in Figure 3.

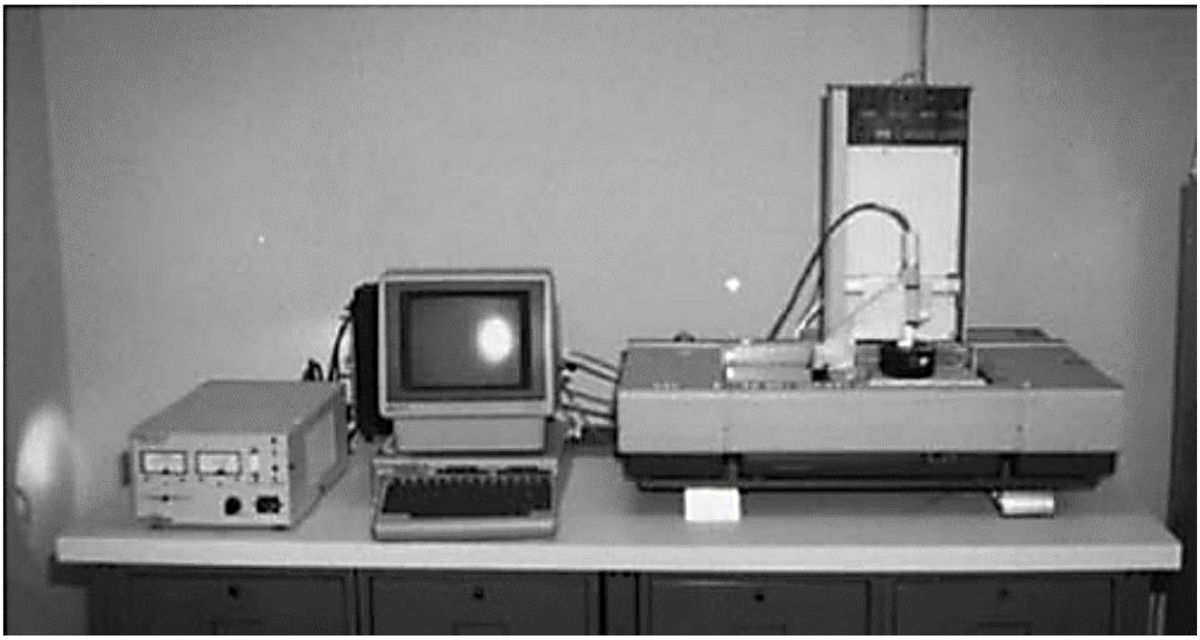

Figure 3. First AM machine produced by the founder of 3D Systems, utilizing stereolithography (Gibson *et al*., 2010).

1.1 Thesis overview

This thesis was prepared to cover important design considerations that need to be addressed in the specific mission profile and further defined manufacturing methods as well as materials utilized. One focus point was on planetary protection (PP) requirements for this mission type, which assisted in selecting an experimental framework to be done during this thesis. With these presented results and findings, this provides an insight into good practices and feasibility of implementing the processes involved in complying with PP requirements. This thesis focused on a mission, to the unexplored surface of Enceladus, an icy moon of Saturn.

The selected manufacturing method for this thesis was AM, which has promising advantages when looking into space missions. It is especially beneficial to understand the PP requirements and their implications on the project flow. This early on intervention will prevent unpredicted delays in project delivery to the customer further along. Since a new era of CubeSat exploration, many companies might be unfamiliar with PP.

The results from the experimental study confirmed the ability of cost-effective bioburden control in achieving certain bioburden reduction levels. In this thesis, dry-heat (DH) was selected as the applicable bioburden reduction method. A heated temperature-humidity chamber with adequate heating capacity was needed.

Importantly the main research questions answered were:
How to assist agile space companies in understanding bioburden control in an additive manufacturing framework by adding awareness and providing a practical experiment?

Can a desktop size 3D-printer materials withstand dry heat bioburden reduction in an environmental chamber?

1.2 Background and motivation

The long-standing self-interest in space and aerospace alike drove the interest of the author in this specific direction. Possibilities for studying space technology in Finnish universities have provided a solid knowledge base for pursuing these research efforts. Finland has had a growing market share in the space industry, as new start-ups and mid-sized businesses are arising. There is extensive expertise available both in the research community and the industry to benefit these new-comers in the field. Global co-operation is necessary for the advancement of space exploration.

1.3 Research objectives

The objectives of this thesis are:
To assess the design for the additive manufacturing process and define additional considerations necessary for a planetary mission with bioburden requirements.

To experimentally assess the suitability of a space resistant material for a selected bioburden reduction method.

1.3.1 Theoretical part

In the theoretical part of this thesis, state-of-the-art knowledge was gathered for each subject matter. The essential background knowledge was acquired to present practical design considerations effectively. It was necessary to understand the design processes generally utilized with AM, feasible AM materials suitable for space, AM as a manufacturing process, and lastly, the available bioburden control methods applicable to the selected material and manufacturing technique. Sources were carefully evaluated, and reliable sources preferred when gathering current information.

Requirements for polymeric materials considered in this thesis included:
- ability to hold mechanical strength and dimensional accuracy after treatment
- bioburden reduction compatibility
- tolerance for radiation in space

- outgassing characteristics in compliance with CubeSat-standard
- availability for desktop size ME 3D-printers.

All the above mentioned were satisfied within the limits of available data. Mainly specific outgassing characteristics had limited data availability, as small variations between manufacturers and batches affect the quality of the raw material.

To ensure compliance with the PP policy, it was not straightforward to determine requirements. This thesis did not focus on determining the bioburden level pre- and post-treatment. Therefore, the minimum criteria were selected as follows:

- dry heat temperatures shall be >125 ºC
- a single dry heat temperature shall be used
- a 5-log reduction in the sterility assurance level (SAL)
- initial surface cleaning shall be performed with isopropyl alcohol

1.3.2 Experimental part

A standard test specimen was designed and manufactured according to standards for tensile testing, to add a practical example on top of the discovered theoretical knowledge. The batch was manufactured and post-processed with a bioburden control method. A single temperature was selected for the post-process due to the long exposure time. Requirements set by the space environment and bioburden process compatibility were considered when selecting materials. While designing the test specimen, design for additive manufacturing (DfAM) approach was followed to ensure proper manufacturability.

A desktop-sized 3D-printer was used to produce a batch of final test specimens. The use of a commercial 3D-printer demonstrated the capabilities of cost-effective solutions available for a wider audience. The test specimen was placed in a controlled environment with a suitable temperature for bioburden control. The temperature of the chamber was controlled during the treatment process. The chamber had been calibrated to ensure suitable levels of accuracy and is, therefore, able to exhibit satisfactory levels of reproducibility.

The processed specimen was placed in a tensile test machine, which had been calibrated. Test results are presented in this thesis, together with pre and post-dimensional measures taken with calibrated measuring equipment.

1.4 Enceladus

Approximately eight astronomical units (AU) away from Earth, but still within our Solar System, it is possible to observe a giant planet visible from Earth via optical telescope. It is the planet with its many rings, Saturn, and orbiting this massive planet are multiple moons. Included in this group is a 504 km diameter icy moon, named Enceladus. First discovered by William Herschel in the late 1700s, it is named after a giant from Greek mythology (Porco *et al.*, 2006). Later in 1981, the first flyby was made by the Voyager-mission, leading to the discovery of the radius of the moon (Pang *et al.*, 1981).

Ever since the ancient Greeks, humankind has been wondering about life existing outside of our pale blue dot. Whether the found life forms are thought to be intelligent or simplistic, is a matter of debate. In the 1900s, the well-known Fermi Paradox and Drake Equation were set forth by physicist Enrico Fermi and astronomer Frank Drake. Both of these ideas tried to bring insight to the question, is there life outside Earth and what the probability of its existence would be (Prantzos, 2013).

With one of the global missions to Saturn´s planetary system, a closer look at Enceladus has been possible and confirmed that ice water had been continuously pluming out of the moon. The particular mission in question was Cassini-Huygens, which was retired in 2017 after nearly 20 years of scientific discoveries, total mission time. (Porco *et al.*, 2006) A pair of captured images are presented in Figure 4.

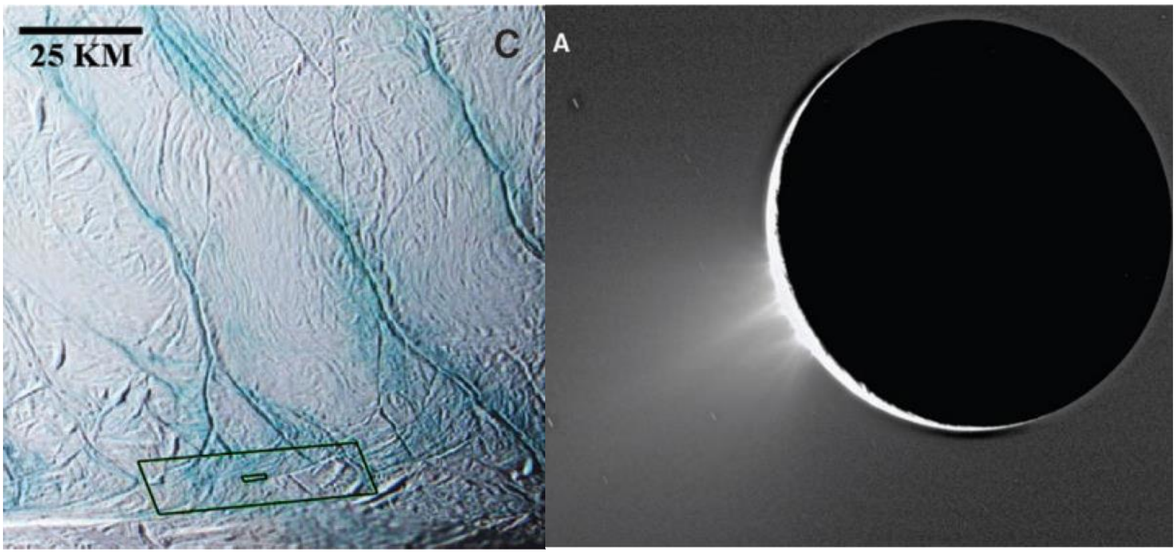

Figure 4. (Left) Icy tiger stripes on Enceladus in false-negative color. (Right) Plumes ejected from its pole. (Porco *et al.*, 2006)

Earlier images were produced in the Voyager 2 mission, and one can be seen in Figure 5.

Figure 5. Voyager 2 images of Enceladus taken in 1982 (Smith *et al.*, 1982).

Further missions have been under analysis, and many types have been proposed to agencies worldwide. As one can imagine, the ideal mission profile would include all types of exploration activities, including landers, orbiters and sample return (Porco *et al.*, 2017). Each activity would focus on searching for specific signs of life and further study Enceladus. However, realistic expectations of a mission realizing all-in-one would require effort to accumulate such financial support to enable this sort of mission. Unfortunately, the limited resources available limit the scientific community. The scientific community has still been able to pursue and expand the knowledge of humankind in any case. The author has had no doubt that humans will soon be exploring Enceladus again, as it is only a matter of time.

2 PLANETARY PROTECTION

The importance of ensuring the viability of scientific discoveries is key to achieving the goals of these efforts when extending scientific interests into extraterrestrial subjects. The means of compromising these studies, especially those related to life detection, is simple when the understanding of micro-organism migration to flight hardware is not understood. While we, as humans, can explore these planetary bodies, we also can contaminate them and therefore disturb the possible life on a specific target. (Kminek, 2018) As was described in the mid-1900s by Feynman (1955), *"To every man is given the key to the gates of heaven; the same key opens the gates of hell."*. This proverb has been a problem of scientific discoveries on many levels and describes the possibility of both discovering and destroying. This proverb has originated initially from the Buddhist religion. Though, in this case, the actual effect is the loss of scientific evidence, it is crucial to understand the implications of our actions.

The search for life will continue forward, even though it has yet to be discovered on extraterrestrial objects. It has proved to be a multi-generation effort even to find the humblest life forms existing in our neighboring planets, and it might likely be that evolved species will remain unfound. The scientific community has still been active, as the Saturnian moon Enceladus is one of the prime candidates for finding evidence of life beneath the global oceans under its icy-shell (Porco *et al*., 2017). One of the reasons for the interest in this icy moon is the observations from the early 2000´s mission Cassini which confirmed water plumes ejecting from the southern pole of Enceladus (Porco *et al.*, 2006). Figure 6 presents the images of the plumes from 2005 can be seen.

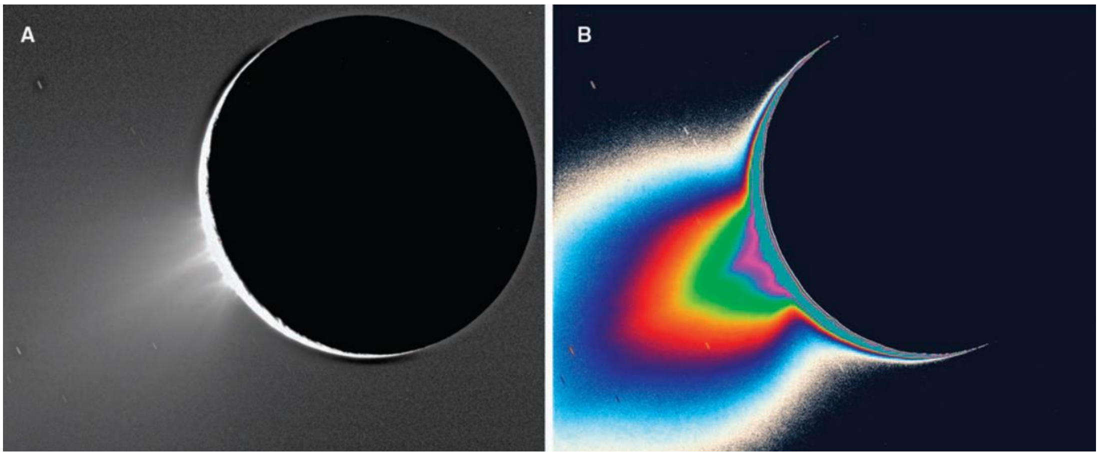

Figure 6. Water plumes ejected from the southern pole of Enceladus (Porco *et al.*, 2006).

In the context of PP, Enceladus holds such a high probability of life that it is classified as one of the highest PP levels set by COSPAR. With the categorization running from levels one to five, the category for Enceladus is set to either three (III) or four (IV) depending on the mission profile. It is possible to make flyby or orbiter type missions to the vicinity of Enceladus in category III missions. These missions require certain levels of bioburden control and documentation of the efforts to ensure suitable protection levels. With both mission categories, it is required to demonstrate a probability of accidental contamination of an Enceladan ocean to be less than $1x10^{-4}$ during the specific mission. Bioburden reduction methods should also be specific to the target body and take to special consideration such organisms that could migrate and survive in the Enceladan environment. Moving to category IV missions, which includes landing a spacecraft on Enceladus, the documentation and bioburden control required are increased substantially. The category IV mission will likely require most of the procedures listed below, in practice(Kminek *et al.*, 2017):

- biasing of the spacecraft trajectory
- cleanroom utilization in multiple phases
- reducing the bioburden
- limited sterilization and bio shielding of immediate contact hardware.

The following parameters are required to be evaluated, when trying to understand further how the probability of accidental contamination is calculated, at a minimum(Kminek *et al.*, 2017):

- bioburden count at launch
- survivability of contaminant organisms during the cruise phase

- radiation effects on organism survivability near Enceladus
- probability on landing, in case of flyby or orbiter
- how and how fast contaminants could reach the liquid water environment subsurface
- probability of the organisms surviving pre- and post-transfer to the subsurface.

The PP policy has yet to specify further requirements to life search missions with landers, as exploration activities have yet to approach the surface of Enceladus. In 2017 it was described that further refinement would be provided in the future years. When looking at requirements for regions of Mars with expected life, much more detail of spore count limitations, both total and per square meter, are available (Kminek *et al.*, 2017).

In addition to the PP policy, most space agencies have prepared documents describing further procedures and practical standards to assist in achieving the required PP levels when considering missions to specified target bodies. Some of these are listed below provided by NASA:

- NPR 8020.12D: Planetary Protection Provisions for Extraterrestrial Missions
- NPD 8020.7G Biological Contamination Control for Outbound and Inbound Spacecraft
- NPI 8020.7: NASA Policy on Planetary Protection Requirements for Human Extraterrestrial Missions
- NASA-HDBK-6022: Handbook for the Microbial Examination of Space Hardware
- NPD 7100.10E: Curation of Extraterrestrial Materials

At the ESA similar documents are available and are listed below:

- ESSB-ST-U-001: Planetary Protection Requirements
- ECSS-Q-ST-70-53C: Materials and hardware combability tests for sterilization processes
- ECSS-Q-ST-70-54C: Ultra cleaning of flight hardware
- ECSS-Q-ST-70-55C: Microbial examination of flight hardware and cleanrooms
- ECSS-Q-ST-70-56C: Vapor phase bioburden reduction for flight hardware
- ECSS-Q-ST-70-57C: Dry heat bioburden reduction for flight hardware
- ECSS-Q-ST-70-58C: Bioburden control of cleanrooms

Of which the ECSS-Q-ST-70-53C provides an overview of methods either studied or used. Various methods of sterilization can be seen in table 1, and to maximize flexibility, multiple methods can be combined to suit the mission at hand. Some of these have been included in mission studies to category IV targets, such as one to Europa, a Jovian moon, or currently utilized in on-Earth medical applications (Imken *et al.*, 2016).

Table 1. Some standard methods for sterilization of spacecraft (ESA Requirements and Standards Division, 2008a).

Type	**Methods**	**Sterilization type**		**Heritage**	
		Surface	**Bulk**	**Studied**	**Studied and used**
CHEMICAL	Formaldehyde gas	X	-	Space components (US 1968)	-
	Ethylen oxide (EtO)	X	-	-	Ranger 1961/62
	Sporicidal solution (TBD)	X	-	Mars 96	Mariner Mars 1971
	Hydrogen peroxide	X	-	-	Mars96, Beagle2, DS2
THERMAL	Dry Heat	X	X	-	Viking, Mars96, Pathfinder, Beagle2, MER,
STEAM	Steam (space hardware excluded)	X	-	-	Excluded on space h/w, only GSE, garments
RADIATIVE	Gamma / Beta radiations	X	X	-	Mars96, Beagle2

Both agencies have made the mentioned publications available online and should industry want to implement specific standards, and it is possible to access it openly. Though every project requires individual assessment of requirements ahead, an overview can be obtained from these documents. One of the first missions to implement broad PP requirements was the Viking mission in search of Martian life, seen in the assembly in Figure 7.

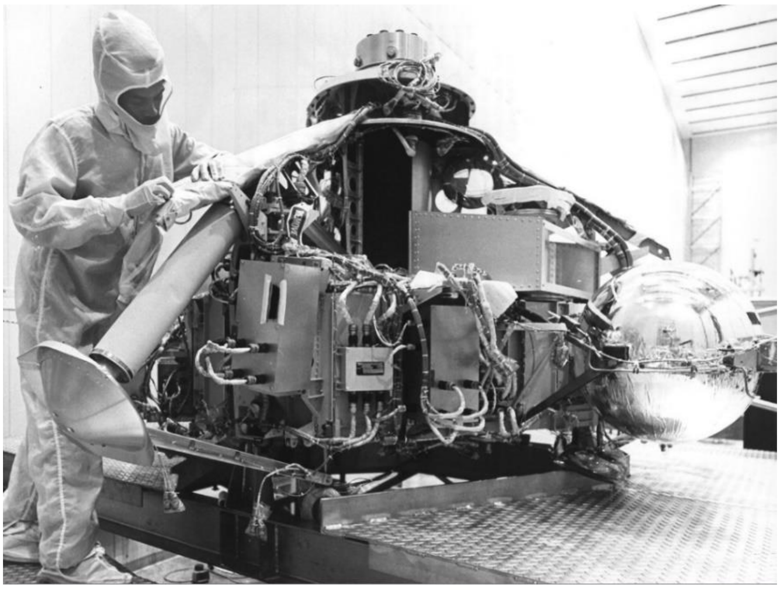

Figure 7. Pioneer of PP in 1975, the Viking mission to Mars (Meltzer, 2011).

2.1 Mission characteristics

As with any space mission, the driver is the scientific goals set together by the public and scientific community. In this thesis, the driver was determined to be the search for life on the surface of Enceladus. While it has been possible to study Enceladus via remote measurements and various imaging techniques, the multiple scientific discoveries await on the surface and below. In previous missions, such as Cassini, measurements of the evidence of life have not been proved due to lack of instrument sensitivity. Such remote measurements would require instrument capabilities providing information, of the oceans, at least of the following (Reh *et al.*, 2016):

- pH levels
- redox state
- available free energy
- temperature.

Each of the listed data points together would provide an overview of the possibility of discovering life on Enceladus (Reh *et al.*, 2016). The current understanding of Enceladus´ subsurface is represented in Figure 8, also illustrating the areas of most significant interest near the South pole. Investigating these characteristics could assist in providing a solid case for an actual surface mission, which is currently being discussed in this thesis. Though the mechanisms of detecting life are not at the center point, it was thought to be essential to understand the current efforts in the field.

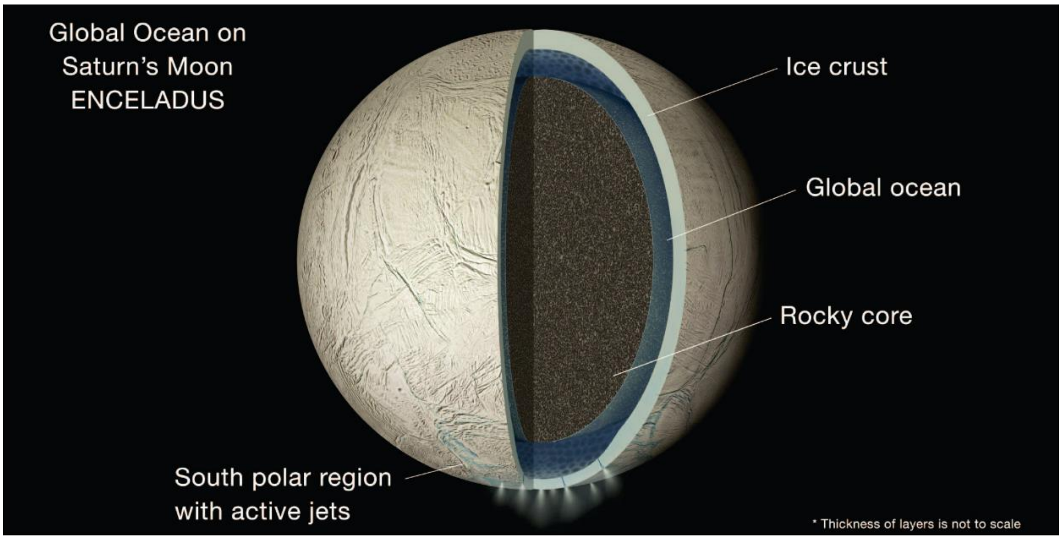

Figure 8. Illustration of the subsurface layers of Enceladus according to current knowledge (Reh *et al.*, 2016).

Some studies have been made mainly based on orbiter type missions, which might be thought to be due to a couple of facts firstly the uncertainty of finding life risk vs. reward and secondly the difficulty of reaching attractive targets beneath the surface. These studies provided some necessary information that is useful when considering any missions that reach Enceladus. One of the mission studies provided by Jet Propulsion Laboratory (JPL) of NASA, is the Enceladus Explorer. In the study, critical parameters used for the mission design, for example, cruise duration to the Saturnian system and the proximity of Enceladus. The proposed mission would orbit Enceladus for a finite period, varying depending on system status upon arrival (Spencer and Niebur, 2010).

In the proposed Enceladus Explorer mission, the entire mission has a planned duration of 13 years from launch to end-of-life (EOL). Of which, the last 12 months would be utilized for orbiting of Enceladus; however, in this case, it would be assumed to be the surface operations duration. Due to the difficulty of reaching the surface, the available mission time on the surface might be thought to be shorter in this case. Nevertheless, the duration of the mission is a representation of the challenges facing any approaching spacecraft. (Reh *et al.*, 2016)

From a PP point of view, the extreme temperatures faced on the surface, at cryogenic ranges reaching 80 K, might be able to provide some benefits by limiting micro-organism survivability (Mitchell *et al.*, 2018). On the other hand, it poses further restrictions on materials selectable for AM processes during design. However, there still are some materials that exhibit consistent performance under these extreme conditions, primarily friction-related properties could be enhanced according to a source (Hecthel, 2014).

2.2 Bioburden reduction and sterilization

Bioburden reduction or sterilization can be used to reach acceptable bioburden levels. Bioburden reduction means reducing the amount of present microbiological organisms, or contaminants, on given flight hardware destined for exobiologically fascinating planetary bodies. Standard methods for reduction, of which a chemical and thermal method were selected for further explanation in the following chapters. The chemical method was chosen to be vapor hydrogen peroxide (VHP) treatment, which consists of applying a vaporized hydrogen peroxide in a controlled chamber onto the flight hardware surfaces. With the thermal reduction method, dry heat (DH), the flight hardware was subjected to a controlled environment where the humidity and temperature are adjusted as per standard. (ESA Requirements and Standards Division, 2013)

It must be mentioned that there has been skepticism towards the current bioburden reduction methods. In a recent study, it was claimed that the micro-organisms after DH treatment are killed, but the signatures of biochemicals that build them up are not neutralized. Though we can satisfy the PP requirements, it might not remove the possibility of inadvertently finding Earthbound micro-organisms on-board. Additionally, it has been suggested that in Mars exploration activities, the PP policy should instead address specific bacteria that could survive on the planet, and bioburden reduction would focus on these unwanted contaminants (Fairén *et al.*, 2019). For Enceladus activities, it could be helpful to conduct a similar study to determine the actual bacteria needing attention during bioburden reduction. Today the PP policy has not yet specified spore counts but instead addresses inadvertent contamination probability of Enceladus.

When selecting materials for flight hardware, it would be beneficial to understand the available reduction methods to take requirements into account early in the design process. It might be that degradation of mechanical performance is seen either directly during the reduction process or possibly further along with the service life (ESA Requirements and Standards Division, 2008a).

2.2.1 Compatibility Requirements

The difference between sterilization and bioburden reduction is that with sterilization, all micro-organisms are killed during bioburden control. (ESA Requirements and Standards Division, 2008a) In the context of this thesis, the word sterilization was not be used but rather bioburden reduction due to the possibility of remaining micro-organisms post-treatment. While estimating and measuring the micro-organism count would be a necessary part of determining the actual bioburden load, this thesis did not assess the initial and final counts.

Certain limitations apply when selecting the material from the available range of AM materials available. There were several options for bioburden reduction methods to choose from, but the two methods discussed further are chemical or temperature-based methods. The chemical process would have required verified chemical compatibility between the selected material and the hydrogen peroxide used as a reducing agent. For the temperature-based methods, requirements come from the designed use temperatures of the material and possible effects caused when exposed to heat.

2.2.2 Vapor hydrogen peroxide

The use of vaporized hydrogen peroxide (VHP) to sterilize medical equipment has been used commonly. The same method has been applicable to surface bioburden reduction of flight hardware. ESA has prepared the ECSS-Q-ST-70-56C standard specifying the process parameters to obtain certain levels of bioburden reduction. The concentration of VHP in the ambient air is presented by mg/L, and process time is adjusted to obtain the reduction magnitude desired. Some polymers are known to react with VHP, so material compatibility needs to be evaluated (ESA, 2013). The application of VHP was not the focus of this thesis and was presented to describe a standard method, should the process be available for use in a space project.

2.2.3 Dry heat

Selecting a suitable procedure requires an understanding of the process parameters from industry standards. The ESA has prepared the ECSS-Q-ST-70-57C -standard to cover the dry heat (DH) bioburden reduction process. Space companies based in Europe mainly encounter this ECSS-standard, and therefore the equally valid NASA standards were not discussed in this thesis. Standard ECSS-Q-ST-70-53C has detailed information on material compatibility testing with various sterilization processes. A short introduction to DH can be found with values to reach a sterilization assurance level (SAL) of 10^{-6}. Table 2 represents D-values, corresponding to the processing time required at each temperature level.

Table 2. Process times, according to ECSS-Q-ST-70-53C for DH, when the maximum humidity level is 1,2 g/m³. Bioburden reduction with this process is 6-order of magnitude from initial bioburden, represented by the SAL 10^{-6} value (ESA Requirements and Standards Division, 2008a).

T [°C]	D-value [h]
110	22
120	10
125	6
130	4
140	2
150	1

The values in table 2 give only a general view of process times in a strictly controlled humidity environment. A full view of possible process times must be verified from ECSS-Q-ST-70-57C, which covers DH in detail. Bioburden reduction can also be performed in ambient humidity, meaning < 12 g/m³, or even in uncontrolled humidity (ESA Requirements and Standards Division, 2013). Critical selection criteria for applicable DH process parameters can include the availability of DH equipment and materials used for the flight hardware. This thesis focused on performing DH with uncontrolled humidity.

The bioburden level of specific flight hardware can be determined by sampling the hardware with a swab or wipe depending on the surface area. Swabs are determined to be suitable for surface areas < 25 cm^2 and wipes for areas < 1 m^2. Further details on determining bioburden levels can be found in ECSS-Q-ST-70-55C, as this thesis did not focus on sampling (ESA Requirements and Standards Division, 2008b). It was necessary to assume the pre-DH bioburden level before selecting the DH process time. Guidance can be found from ECSS-Q-ST-70-57C chapter 5.2.2.b, which reports that bioburden before reduction can commonly be between $3x10^2$ to $1x10^5$ bacterial spores/m^2 (ESA Requirements and Standards Division, 2013).

Taking the surface area of the test specimen used, $5{,}53*10^{-}3$ m^2, according to CAD-software, resulting in an estimate of 2,00 to 553 bacterial spores on the surface of the specimen. Applying a SAL 10^{-5}, 5-order of magnitude reduction of spores would equal to $2{,}00x10^{-5}$ to $5{,}53x10^{-3}$ spores on the entire surface, providing a decent reduction of spores.

It becomes clear from ECSS-Q-ST-70-57C chapter 5.3.1.2 that humidity control is not required when applying DH processes aiming for 4-6 orders of magnitude reductions, due to increased temperature requirement. The minimum +110 ºC is only applicable to 2-3 order magnitude reduction, and for the higher reductions,> 125 ºC are required. According to the standard, with a temperature between 125-130 ºC, the process time D(hours), in hours, can be determined (ESA Requirements and Standards Division, 2013):

$$D(hours) = 10^{-3.5991+\frac{2049{,}0923}{(T+273)}} \quad (1)$$

In equation 1, the T is the process temperature used for DH. The value obtained from equation 1 represents the 4-order of magnitude reduction, and to reach 5-order magnitude reduction, the value was multiplied by 2 (ESA Requirements and Standards Division, 2013).

In this thesis, the lowest possible temperature to reach 5-order reduction, +125 ºC, was selected to limit the deformation of materials. Calculating the processing time from equation one results in a 35-hour 26-minute, further multiplying this by 2 to obtain 5-order reduction results in a 70-hour 52-minute process time.

Reductions in process time can be achieved by increasing the temperature. However, the used thermoplastics start to deflect with varying temperatures above +100 *ºC*, limiting possible process temperatures. The polycarbonate (PC) filament datasheet declared that the glass transition temperature is +112 *ºC* which was lower than the process temperature. The heat deflection temperature was not reported, but the maximum service temperature is +110 *ºC* (Ultimaker, 2018). The reason for selecting the higher temperature is that a pure PC sheet is declared to have a glass transition temperature of + 145 *ºC* and a heat deflection temperature of +132 *ºC* - +142 *ºC* (Arla Plast, 2014). It was suspected that the DH process might cause deformation in the AM PC test specimen. A rigid surface and even cooling were used to limit the probability of warping during the DH process. This type of support might not be possible for actual flight hardware due to complex geometries.

The overview of the bioburden process flow, as described in ECSS-standards for the bioburden reduction process, is presented in Figure 9.

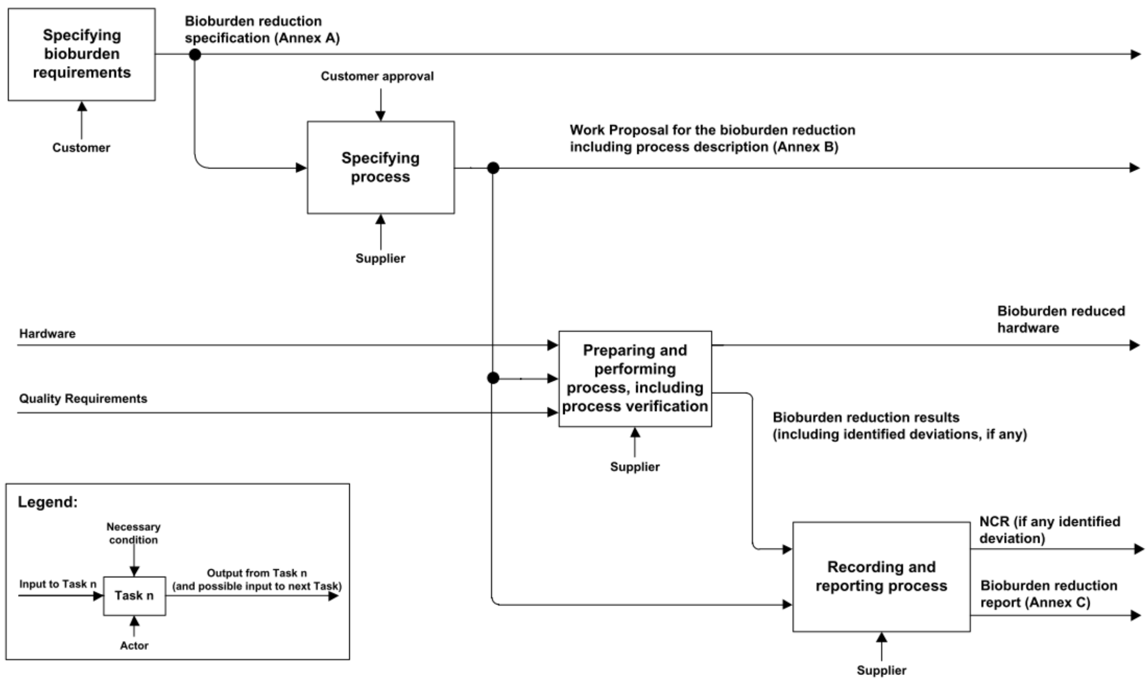

Figure 9. Overview of the bioburden reduction process as described in ECSS-Q-ST-70-57C. The input of the process is the requirements set by the customer, and output is the bioburden report with the required level of detail as set by the standard (ESA Requirements and Standards Division, 2013).

3 ADDITIVE MANUFACTURING

Under the umbrella term of AM, a total of seven different processes exist according to International Organization for Standardization (ISO) and American Society for Testing and Materials (ASTM) common standard 52900. These seven processes are presented in Figure 10. In a scientific framework, the term AM is preferred over 3D-printing, though the latter is used by a broader user base, which is represented by the higher search engine result count for the term “3D-printing” in 2017 (Wohlers Associates Inc., 2017, p. 17).

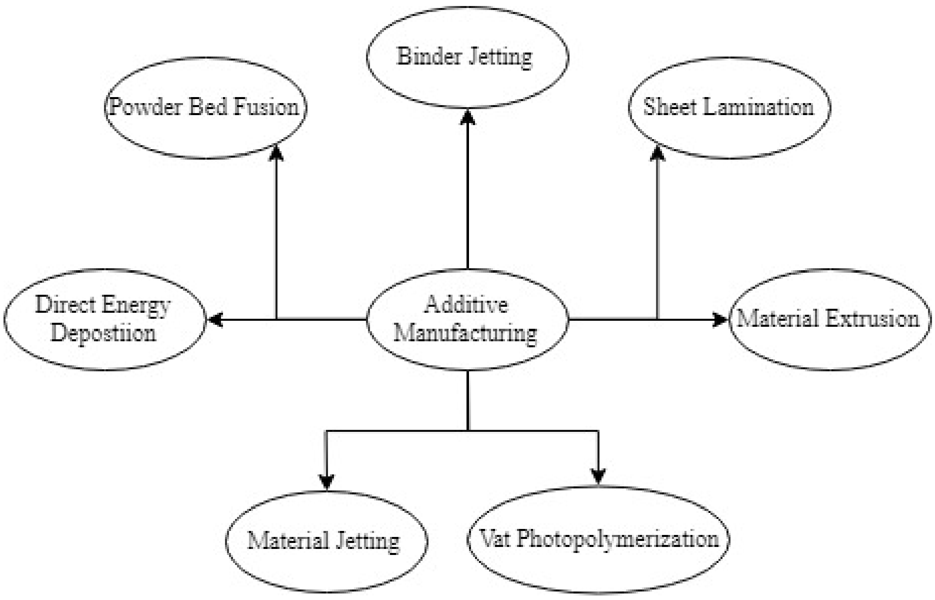

Figure 10. Seven sub-processes defined under the AM framework (ASTM International and ISO, 2015).

In today´s industrial world, AM has been utilized in a range of applications, from functional parts to visual aids for marketing purposes. In Figure 11, the distribution of application areas across the field is presented in a pie chart form. Functional parts have been the dominating end-use application for AM applications today, which suggests that the maturity of AM parts is enough to perform specific functional tasks. It must be noted that less than one-third of the applications are for visual or educational, meaning that over two-thirds are used in other supporting functions for manufacturing or functional parts. The presentation models, visual aids, other, and education/research are thought to be purely visual or educational in this context.

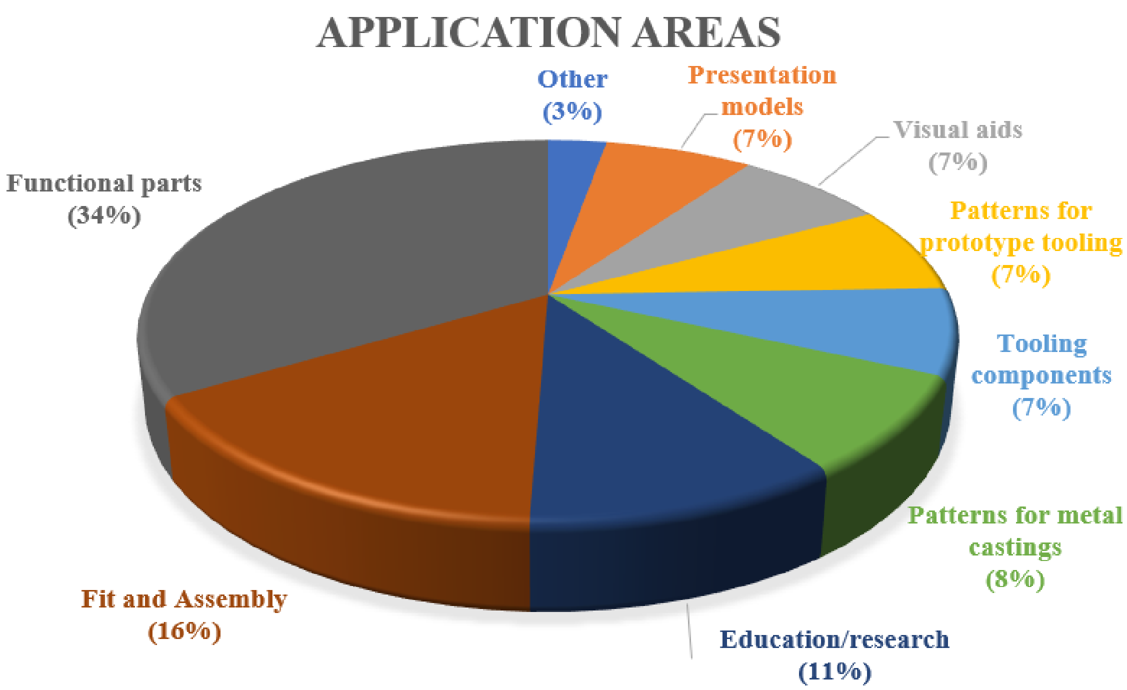

Figure 11. Application areas of AM in order of percentage, based on a survey reported in 2017 (Wohlers Associates Inc., 2017, p. 24).

Such functional parts are taking advantage of the benefits provided by AM. Creating complex shapes impossible to manufacture using traditional manufacturing methods and the extended possibility to optimize structures enable many industries to achieve the lightweight and high mechanical performance parts required. Industries with mass-critical end-products, such as aerospace and space, have been able to implement AM in a wide variety of parts (Morretton *et al.*, 2019). Manufacturing parts that hold an optimal mass to performance ratio can drive the cost of space exploration down with decreasing the need for fuel on-board. This can be seen in Figure 12, where the aerospace industry represents one of the top industries utilizing AM. It was assumed that aerospace also includes the space sector as well.

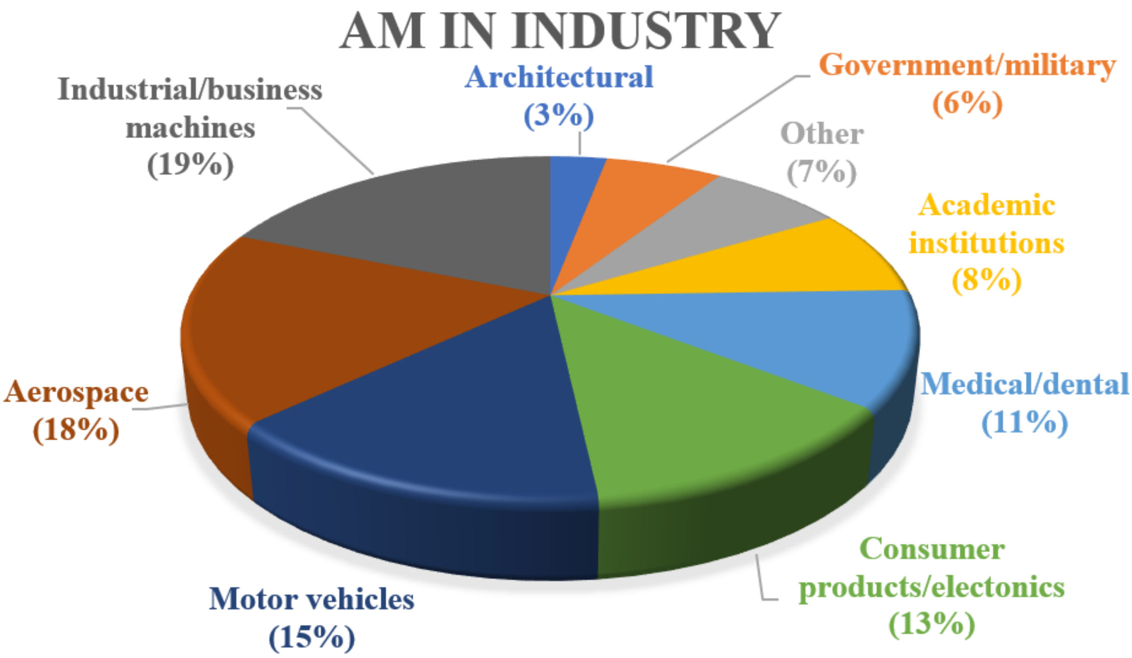

Figure 12. Comparison of AM utilization in various fields of industries in 2017 (Wohlers Associates Inc., 2017, p. 22).

Through the global market, manufacturing companies have been facing increased pressure to produce new innovative products with a short time to market. Therefore, it has been essential to reduce the used time on design, manufacturing, and testing. This flexibility has not been not achievable through traditional manufacturing, which commonly requires long production times and tends to use excess energy to subtract material from the workpiece, causing waste. Currently, AM applications tend to be highly customizable end-products, which have been produced in small scale series. Large production series tend to have favored the traditional methods due to faster production time per part, once a significant initial investment of time and money has been spent. This has brought an edge to AM, as complexity and rapid changes can be implemented into manufacturing with reasonable effort. In traditional manufacturing, time and cost of manufacturing have grown exponentially after a certain level of part complexity is achieved. Furthermore, some geometries have been impossible to create with, for example, machining or casting and this is when AM can be considered as an enabler. Figure 13 presents the cost versus complexity that can be seen, which highlights the advantage of AM (Chua *et al.*, 2017, pp. 2-3).

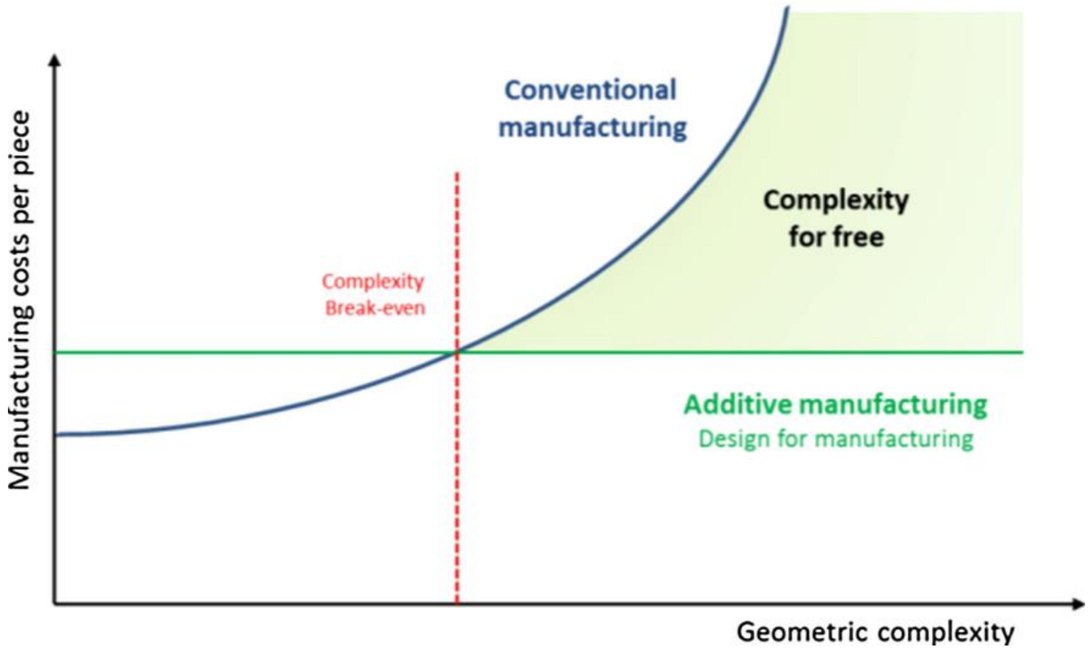

Figure 13. Cost of manufacturing in comparison with the increasing complexity of part geometry, representation of AM complexity benefit. Graph derived by Kirchheim *et al.* (2017) from Hopkins and Dickens (2003).

The design verifications can be made with a decreased lead time before releasing any products into the market. This flexibility has meant improvements, for design errors, have been possible to be implemented rapidly, and new parts could have been printed one after another, which represents an agile process used in the Formula One racecar design. In the field of aerospace production, lead times can be up to 60 weeks, which has meant slow developmental efforts. Applying AM, in this case, was reported to enable lead times in a time frame of one month. (Chua *et al*., 2017) The agile process of AM is visualized in Figure 14.

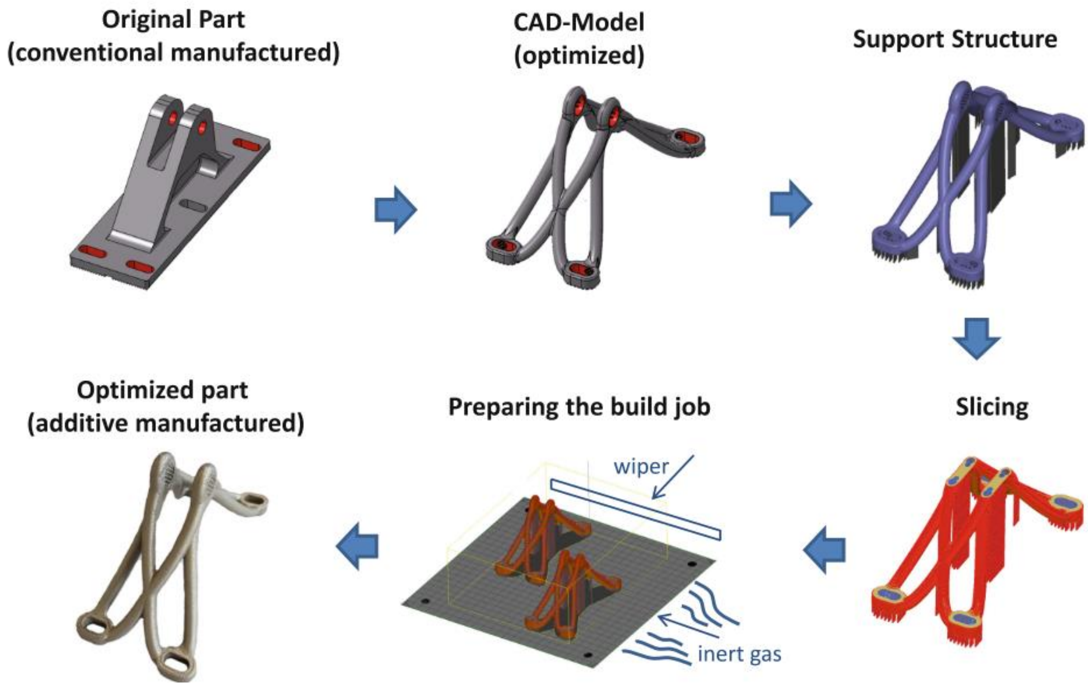

Figure 14. Design capabilities utilized in AM for fast iteration (Kirchheim *et al*., 2017).

The global manufacturing market was estimated, in a 2017 report, to be approximately 12 trillion USD. Of this market, AM has had a share of approximately 6 billion USD, leading to only a 0.047% share of the entire market. Reportedly, AM should grow into a 26 billion USD market by 2022, meaning a market share of 0.217%. While the figures might seem minuscule at this point, the growth potential for AM has been high. Careful estimates have been suggesting a 5% market share could be obtained in the future. (Wohlers Associates Inc., 2017, p. 297) Aerospace was predicted to be one of the leading industries in this growth due to the demand for lighter weight, higher strength, and durable parts (Kumar and Nair, 2017).

The versatility of AM can provide support in all areas related to aerospace, to support industry growth. Whether they are functional parts for a Mars rover of NASA or tooling related to its manufacturing processes, these limited and complex needs can be met by AM.(Chua *et al.*, 2017, pp. 11-12) Choosing AM over traditional methods in any process has been a complex task involving many considerations. If the product represents multiple characteristics listed below, AM could have outperformed traditional manufacturing in many cases (Gaudenzi *et al.*, 2018):

- customization required

- extensive development time
- the high complexity of geometry
- mass savings
- multiple component/part construction
- multiple iterations in design
- performance requirements high.

These requirements have often been faced in the space industry. Therefore, AM has proved to be particularly useful. Once a product has been evaluated to be a suitable candidate for AM, a material selection needs to be made. Depending on the available equipment and part requirements, the selected material may be polymer, metal or a hybrid. In today´s world, the dominating materials have been polymer-based. Though specific applications mandate metals, due to structural strength and other material properties, polymers have still been able to perform specific tasks. The distribution of AM material use is presented in Figure 15.

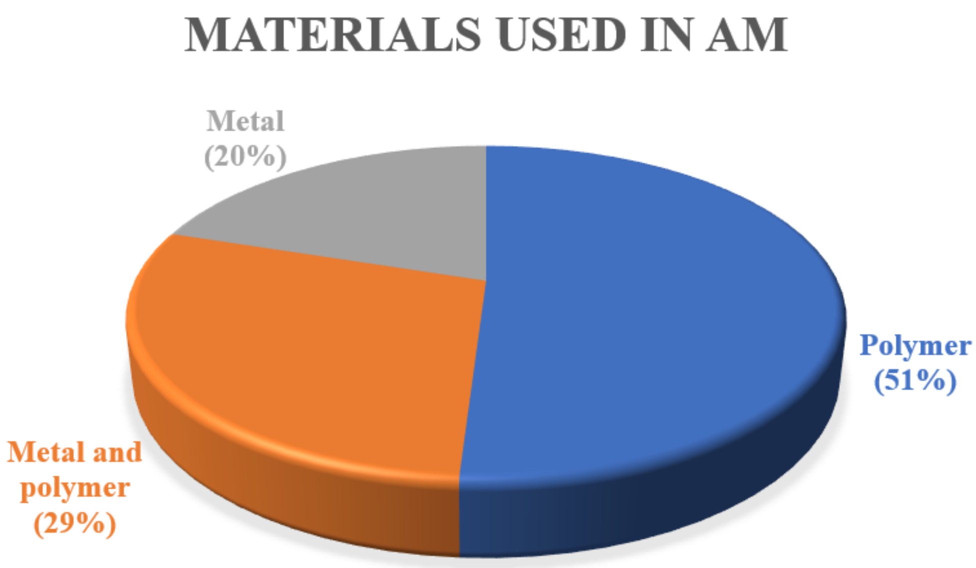

Figure 15. Material utilization in AM (Wohlers Associates Inc., 2017).

3.1 Design process

The word design has been described as a process in which steps are taken from an abstract concept of an object to a refined and detailed description of the object, eventually enabling manufacturing. The process moves forward to modifying the information and finally providing enough information to have produced the object, beginning with the initial information available. The drivers of design have been characterized as design problems that specify an information gap that is required to be fulfilled. As an example, it could have been determined that a beam is to be designed, but the shape of the beam, for example, I-beam or any other shape, is unknown at that point (Poli, 2001, p. 1).

The design process for traditional manufacturing methods has been shifting towards AM focused design, similarly to the evolving design process of entire small satellites (Madry *et al.*, 2018). The design for manufacturing and assembly (DfMA) framework has, therefore, been replaced by design for additive manufacturing (DfAM). This change in design framework has been due to different limitations applying to AM in contrast with traditional manufacturing leading to the new design framework (Booth *et al.*, 2017).

Utilizing of AM in today´s manufacturing world has been limited partially by the creativity of designers. With the long-standing experience with traditional manufacturing, it has created some creative constraints in the minds of designers. To fully take advantage of AM, it has been necessary to understand what might previously have been impossible, could well be realized with AM (Hällgren *et al.*, 2016). The rapid increase of accessibility to AM, for example, in classrooms or public areas, has led to designs created by all levels of expertise. (Booth *et al.*, 2017) This increased accessibility has been promising to observe, as a new design mindset has evolved naturally.

3.1.1 Design for additive manufacturing

While DfAM has still been evolving, research on the subject has tried to determine what DfAM is and how it is expected to help designers. The development of DfMA in the 1980s provided to be an essential driver in the development of current design methodology. It has been expected that DfAM should provide a similar ground and further enhance the capacity of the designer community (Boschetto *et al.*, 2019).

The DfAM has not yet been defined; however, some attempts have been made. Figure 16 presents a closed-loop design process enabled by DfAM is presented. Due to the complex nature of AM parts, it has been stated that it is challenging to create a design framework that guides designers to utilize the full potential of AM. In this proposed DfAM design framework, a generic process flow has been attempted to be captured to suit a variety of AM processes. Modern computer-aided tools for designers have been refined over the years to suit traditional manufacturing, which is yet to enable incorporation of AM in the design phase fully. A full design for AM toolbox has yet to have been developed, but optimization tools can assist in utilizing the potential of AM. The efforts to assist designers in implementing AM in the design phase currently rely on case studies, which have brought insight into the possibilities. Due to the sophisticated capabilities provided by AM, at some point, it will have been necessary to develop DfAM related training further. It might be useful to specify specific limitations with each AM process, for example, a minimum wall thickness achievable. However, this might be highly machine and material-specific, further complicating the development of generic instructions for AM designers. (Fu *et al.*, 2018)

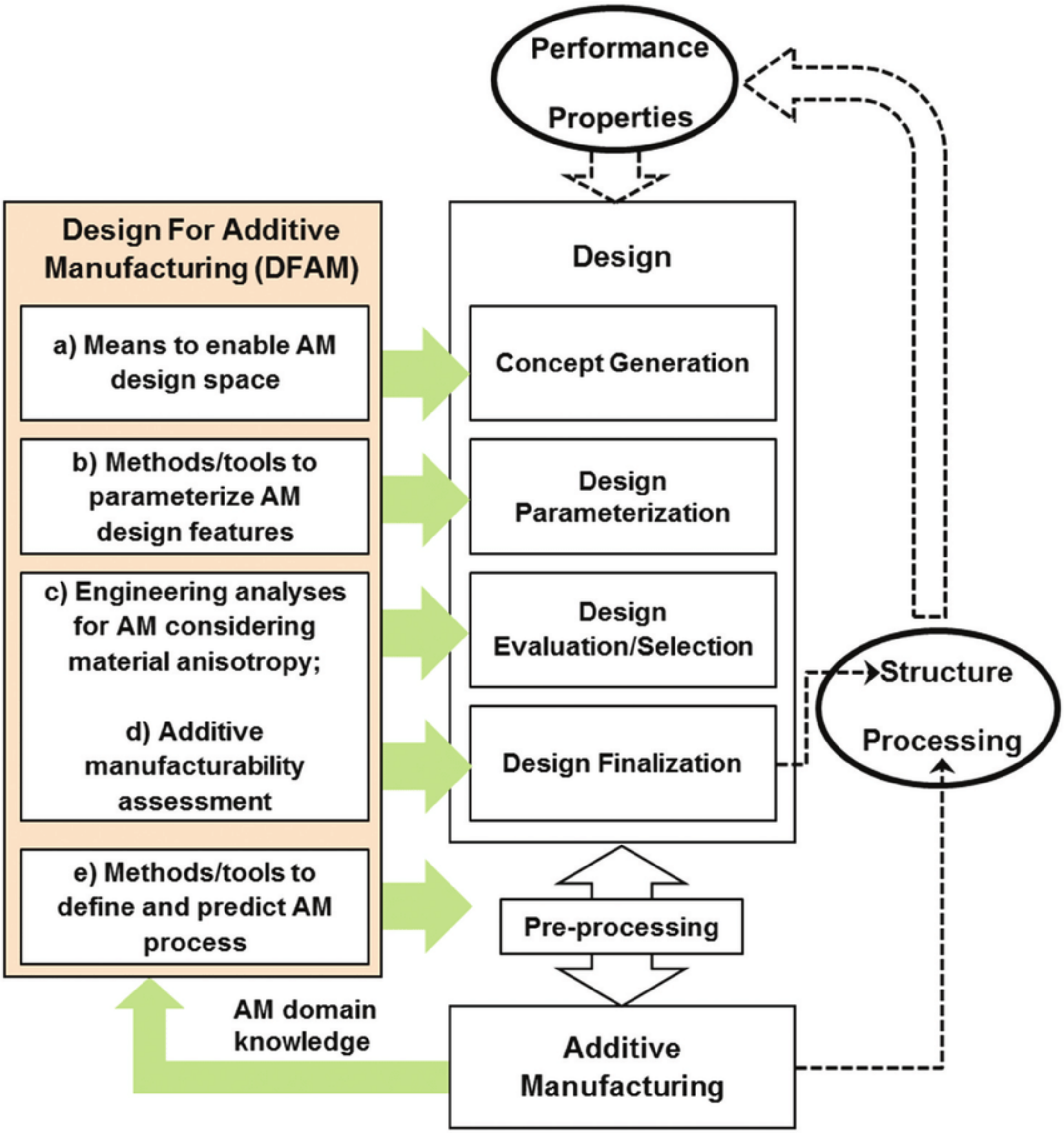

Figure 16. DfAM enabled design framework, a closed-loop approach (Fu *et al.*, 2018).

3.2 Use cases

Real-life space use examples of AM were presented in this section applications, both polymer and metal-based. Flight results have not yet been available from many AM applications designed for space use but include only Earth-based observations and tests for space suitability of AM. It has therefore been beneficial to understand the novel designs that were enabled only by utilizing AM.

3.2.1 Xatcobeo and Humsat-D

Multiple missions, involving both CubeSat and more massive spacecraft, have been demonstrating the capabilities of AM in space. The first example has been flight-proven on two separate CubeSat missions, the Xatcobeo and Humsat-D. Both missions were developed at the University of Vigo in Spain, in cooperation with a Spanish National Aerospace Institute (INTA), and promoted by the European Space Agency (ESA). In the initial mission, Xatcobeo launched in 2012, the main goals of the mission were to perform radiation measurements in low-earth-orbit (LEO) and test a newly developed solar panel deployment mechanism developed by INTA. As for the Humsat-D, it was part of a program called HUMSAT aimed towards humanitarian initiatives focusing on developing areas of the world, for example, climate change tracking, remote disaster follow-up, and public health communication. Regardless of the application enabled by CubeSats, the AM perspective in both missions focused on developing an antenna deployment mechanism (Vilán Vilán *et al.*, 2015). Figure 17 illustrates the physical model prepared for the missions, which was identical in both cases.

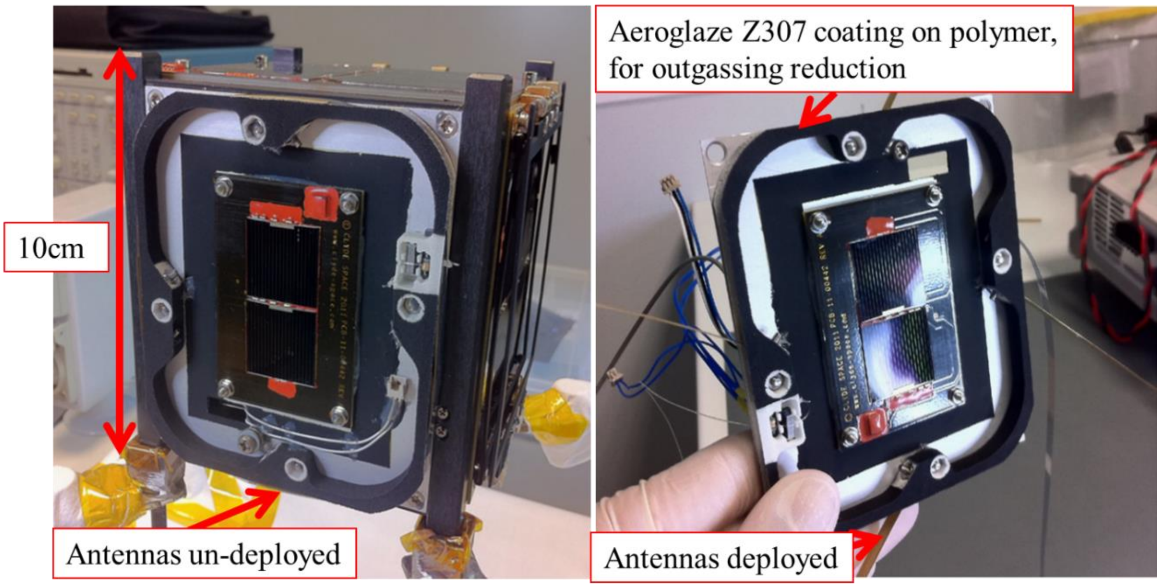

Figure 17. Polymeric AM antenna deployment mechanism used on the Xatcobeo and Humsat-D CubeSat projects (Vilán Vilán *et al.*, 2015).

The antenna in these missions was designed to support communications between the satellite and Earth utilizing an ultra-high frequency (UHF) amateur radio frequency, commonly found in CubeSats. As seen in the deployed condition of the antenna in Figure 17, there has been in a total of four monopole antennas protruding at a 45-degree angle from each side. When designing such structures, a key design factor is the mass of the structure. The mass of the structure or part has been one of the main selection criteria used to go ahead with AM in this use case. While material properties of polymers might be optimal when it comes to outgassing and electrostatically charging environment, the mass has often driven the design to find solutions to enable the use of polymers (Vilán Vilán *et al.*, 2015).

The selection of a polymer for the specific application was also based on the low density and dielectric nature of polymers. After consideration, a fiber-glass reinforced polyamide was selected as the material. The AM process selected was PBF or selective laser sintering (SLS), as referred to in the report. Some advantages and limitations of the material and PBF are listed below, as reported(Vilán Vilán *et al.*, 2015):

- nearly limitless object geometry
- ability to generate multiple prototypes
- material density at 1,00 g/cm^3
- limited material performance
- tolerancing of CAD requires experience.

When designing the sub-chassis for the deployment mechanism, it was required to consider other material requirements on top of the space environment. In the complex structure, there were integrated electronics and heating elements for the release of the antennas. The heat generated during the release phase would have been capable of damaging the polyamide base structure, which required additional engineering. In the final design, a polyether-ether-ketone (PEEK) insert was designed and can be seen in Figure 18.

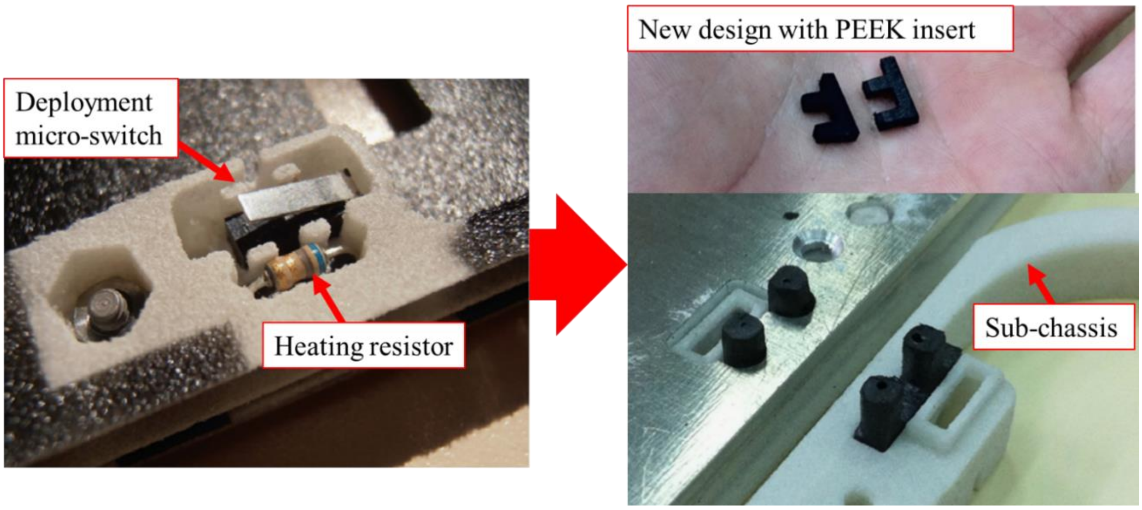

Figure 18. Original design on left, iterative design with black colored PEEK insert for additional heat resistance to prevent sub-chassis from melting under heat load(Vilán Vilán *et al.*, 2015).

During the study, some measurements for the outgassing properties of the selected materials were presented. The tests for the polyamide material had been made in 2004 by ESA, which demonstrated near compliance with the required TML limit of 1.00 %. For the presented Aeroglaze and PEEK values, a source could not be determined, but are still presented in table 3.

Table 3. Outgassing values for Aeroglaze Z307, polyamide 11, and PEEK, as presented in the study (Vilán Vilán et al., 2015).

Material	**TML [%]**	**CVCM [%]**	**Source**
Polyamide, reinforced with fiberglass	0.72	0.01	Estec/544 (QM/3958)
Polyamide, reinforced with fiberglass + resin	1.07	0.01	Estec/544 (QM/3958)
Aeroglaze Z307	1.06	0.04	Undisclosed
PEEK, carbon fiber composite	0.16	0.00	Undisclosed

The referenced Estec/544 report was searched online, but it was not publicly available. It was reported that the study had only been performed twice on the polyamide materials, and therefore limited confidence in the results was mentioned. (Vilán Vilán *et al.*, 2015). Additionally, it was uncertain how the different results from any outgassing test could be applied to materials provided by other manufacturers or even different batches in the coming years. Though variations may be insignificant, they may still be a limiting factor for selection provided outgassing limits are not met. Testing of outgassing can be performed under standards provided by various space agencies; for example, ESA prepared ECSS-Q-ST-70-02C. It has seemed that results from older tests might be adapted or used as a basis for engineering decisions in agile CubeSat projects.

3.2.2 PolarCube

The PolarCube was a 3-unit CubeSat developed by the University of Colorado Boulder to demonstrate atmospheric sounding, detect ocean ice boundaries and map Polar regions. In this 5 kg satellite, a feed horn for the radiometer payload onboard was manufactured using AM. The feed horn acts as a radio signal focusing element, focusing the signal and adding slight gain to the signal. Figure 19 presents the actual feed horn with dimensional details.

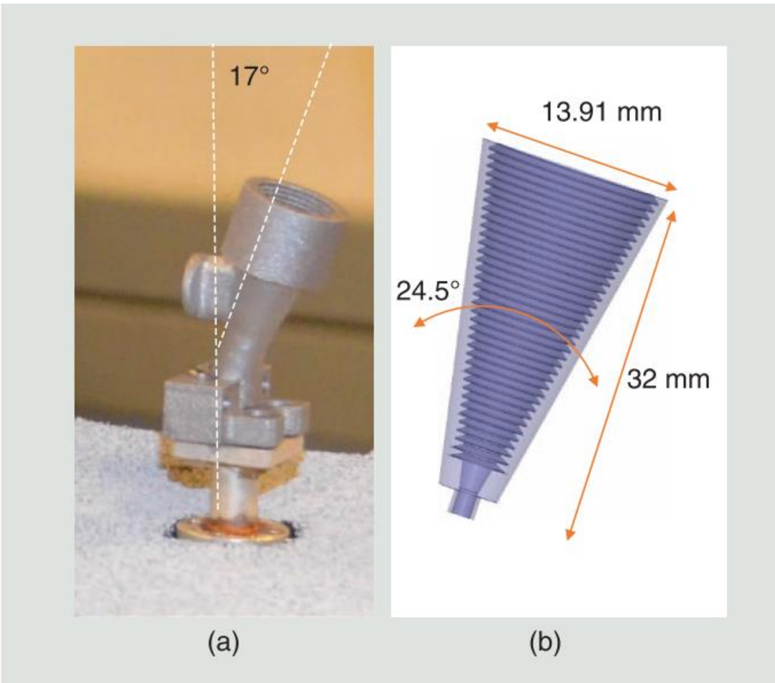

Figure 19. Feed horn developed for the PolarCube utilizing AM from AlSi10Mg with PBF (Gordon *et al.*, 2017).

.

At the time of this thesis, it could not be determined was the PolarCube launched already. It was assumed that it was still under development as any post-launch research articles could not be found.

3.3 Materials selection

Selecting a material for any application requires a basic understanding of its properties. Some essential guidance for engineers, in selecting the suitable material for a use case, can be obtained by considering the following characteristics (Fortescue *et al.*, 2011, p. 256):

- coefficient of thermal expansion
- ease of manufacture
- material conductivity
- material stiffness
- material strength
- resistance to fatigue and fracture.

Though the manufacturability has not been quantitatively measurable, it has been an integral part of the material selection process. The space application discussed in this thesis as unique requirements and focus were given to space suitability and process compatibility. As the materials of interest were in the polymer category, the additional characteristics were to be considered (Muraca and Whittick, 1967, pp. 1-2):

- thermal-vacuum environment effects
- radiation effects
- survivability of bioburden reduction methods.

For polymers being deployed to space, the dominating effects have been caused by the vacuum of interplanetary space, which is in the range of 10^{-15} bar and below (Muraca and Whittick, 1967, p. 2). In these ultra-high vacuum conditions, polymers start to exert gas from both the internal and external surfaces of the polymer itself. This gas exertion has been referred to as outgassing, which can be measured with two parameters. Firstly, the total material loss (TML) and secondly the collected volatile condensable materials (CVCM). The main concern with the outgassing of polymers has been the contamination of adjacent surfaces. Sensitive instruments on-board the spacecraft could be immobilized and lose functionality. This probability of contamination was the reason for standards specifying the TML limit to < 1 % and CVCM to 0.1 % (Grossman and Gouzman, 2003).

The heat effects needed to be assessed due to the DH bioburden control process in this thesis. Critical parameters for assessing the heat effects included glass transition temperature (Tg) and manufacturer recommended maximum service temperatures. Some Tg and tensile strength can be determined from Figure 20, the available AM materials being of primary interest.

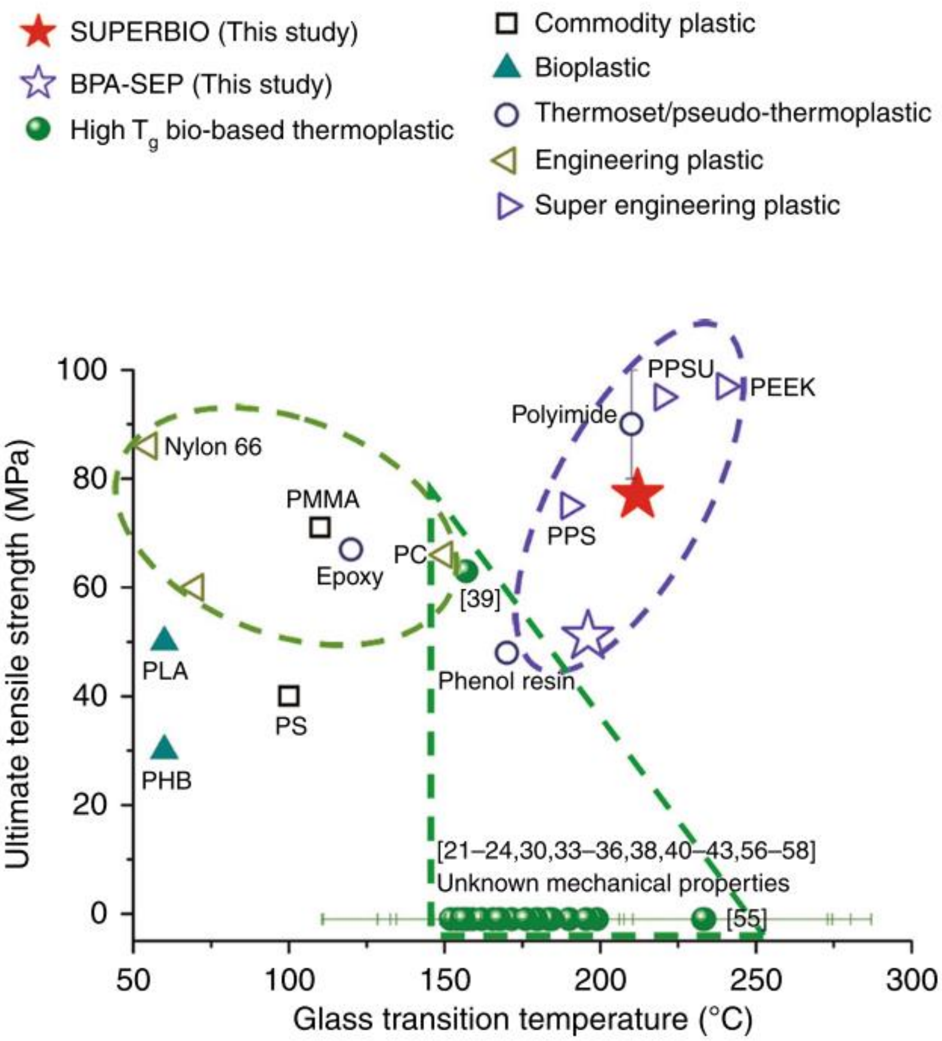

Figure 20. Ultimate tensile strength and glass transition temperature for various polymers, PC, and PEEK of primary interest (Park *et al.*, 2019).

PC was selected due to space-grade outgassing reported and availability for production on ME-based AM machines.

4 AIM AND PURPOSE OF EXPERIMENTAL PART

The purpose of conducting the experimental part of this thesis was to present an actual application of the bioburden reduction method on AM specimens. It was essential to demonstrate what the effects of the dry heat (DH) process are when applied to an AM specimen. The DH was selected, as it was thought to be widely available. Access to a test chamber was a selection criterion, as well. One of the research questions was, can dry heat used as a bioburden control measure to be utilized on an off-the-shelf material available for a desktop-sized 3D-printer.

The basic idea was to provide concrete examples of AM parts with and without application of dry heat. This experiment was thought to provide a comparative view of the mechanical properties that would be encountered when applying the dry heat (DH) process on selected AM materials. All experiments were performed on calibrated equipment to ensure traceability and reproducibility for further studies. Details of each equipment have been provided in the coming chapters.

5 EXPERIMENTAL SETUP

The setup of the experiment required various resources, such as AM machine, tensile test machine, and measuring equipment. The following section discusses all used equipment and the setup used to accomplish the experiment.

5.1 Equipment for milled specimen

The details for the used equipment for milling PC specimens are gathered presented in table 4.

Table 4. Parameters and tools used for milling of PC samples with Rensi CNC-machine.

Model / Manufacturer	Rensi Excitech E2-1530
Machine serial number	1506073

5.2 Equipment for material extrusion specimen

The key idea of this thesis was to provide a practical example were bioburden reduction would be applied. Therefore, it was essential to make test samples with AM and apply the treatment. The first thought was to utilize the AM equipment used at Aalto University Digital Design Laboratory (ADDLAB) of Aalto University located in Otaniemi, Espoo. The reason for this was that there was some previous experience of use, and they could print the selected material. Libraries around Helsinki, Vantaa, and Espoo regions have similar 3D-printers for public use. However, the material selection is limited to polylactic acid (PLA) only though it might be reasonable to negotiate with the libraries to dedicate a printer for experimental or own materials.

The first option was an Ultimaker 3 (UM3) 3D-printer, which represents a higher-end consumer printer retailing in the 3-4 k€ range in Europe. The UM3 is capable of extruding materials requiring nozzle temperatures below 280 ºC. The build plate provides a bed area of approximately 200x200x200 mm in size. While the build plate has heating, the chamber does not. (Ultimaker, 2019a) The printer can be seen in Figure 21.

Figure 21. Option 1, 3D printer at Aalto University Ultimaker 3 (Ultimaker, 2019b).

It was necessary to use an additional heat deflector on the front opening of the UM3 to prevent heat loss due to airflow. The need for heat deflection was based on previous experience on printing PC, obtained from a research project at Aalto University. The top part of the UM3 is open, and excessive heat loss is encountered, complicating the printing of materials susceptible to warping.

The second option provided additional functions compared to the UM3. This printer was more expensive, but it could produce higher temperatures in the chamber, build plate as well as the nozzle. Therefore, the Intamsys Funmat HT (IFH) is capable of extruding materials with higher melting temperatures, up to 450 ºC. The build volume was of similar size as the UM3, with improvements only in temperature performance. The insulation was superior, and the chamber heat can be maintained when the door has not been opened during printing (Intamsys, 2019). Figure 22 presents the IFH at Aalto University.

Figure 22. Option 2, 3D printer at Aalto University, Intamys Funmat HT.

The test specimens were selected to be manufactured from polycarbonate (PC). The main reasons being suitability for space vacuum with a low-outgassing rate and machine selection. Some AM machine manufacturers, such as Ultimaker, have proprietary brands of filament. The variations between manufacturers differ in filament diameter and mechanical properties depending on the compounds found in the filament. This thesis focused on Ultimaker PC with white color, as it was readily available from a local supplier. Other colors were available, and the clear filament had a 22 MPa higher tensile strength at break than the colored filaments according to the datasheet of the manufacturer. The tensile strength was not prioritized at this point, rather the availability and lead time for printing. The manufacturer reported tensile strength at break was tested according to ISO 527, with a 50 mm/min draw speed (Ultimaker, 2018).

Originally it was planned only to produce AM test specimens from PC, but another material was used as well for a single specimen. It was made of polyvinylidene difluoride (PVDF) and recommended by the supplier of the PC specimens, due to its radiation tolerance. The single PVDF specimen was subjected to dry heat. Nile Polymers manufactured the filament, and the commercial trade name was Fluorinar-C Kynar PVDF filament. It was noted that the tensile strength of PVDF was nearly 30 MPa lower than PC. However, PVDF has high resistance to nuclear and UV radiation (Nile Polymers, 2005). The outgassing data available from ESA and NASA both confirmed PVDF to be within TML and CVCM, with 0,01 % TML and 0,00 % CVCM. The ESA test data was from a 2001 test numbered Estec/520. However, the outgassing database had a remark that test data was too old (ESA, 2001). Limited outgassing test data is available, and available data needs to be used as a basis for engineering decisions.

The plans of AM the specimens without external help turned out to be too time-consuming considering the workload conditions at the time. Therefore, a last-minute change was to use an external partner to manufacture the test specimens. A quote was received from Maker3D Oy located in Helsinki, after sending the STL-file and specifying the number of specimens needed. The supplier selection was made after helpful discussion with the staff and availability of an Ultimaker 5 (UM5) 3D-printer in Figure 23, close to the UM3 discussed earlier.

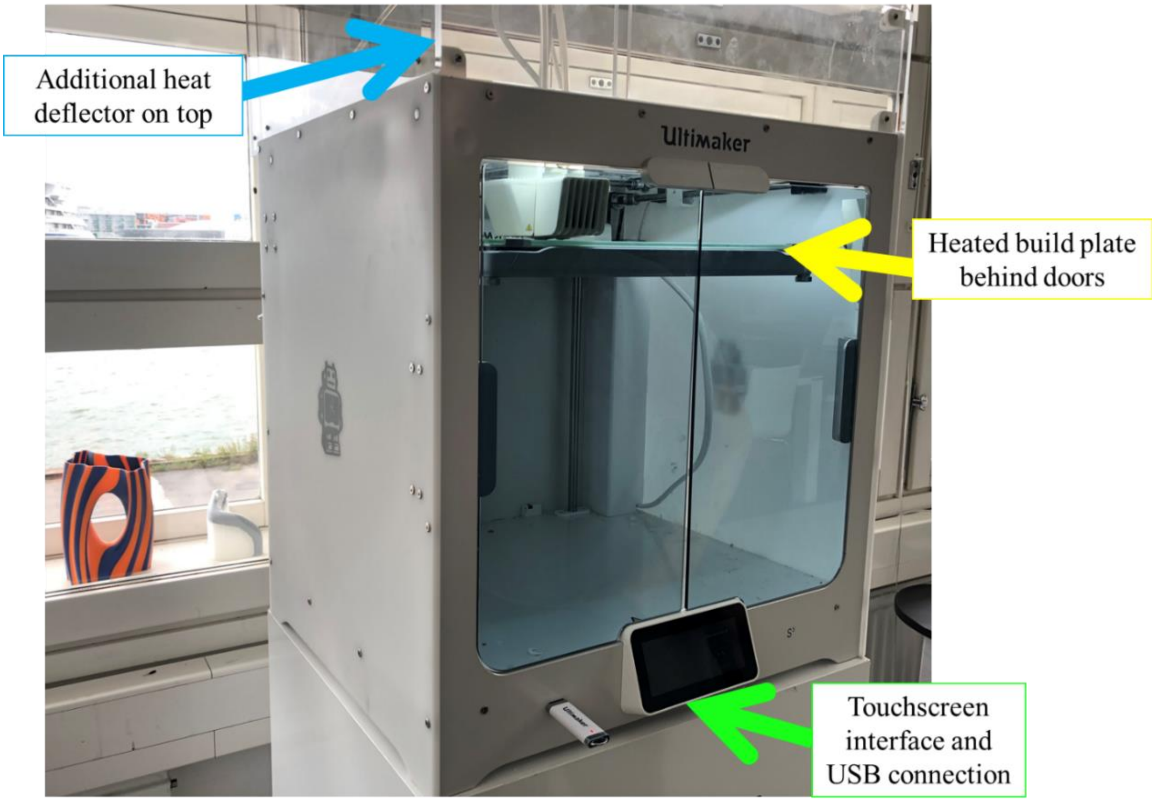

Figure 23. The actual 3D-printer used was Ultimaker 5 at Maker3D facility in Helsinki. Note the additional heat deflector on top, not found on the Ultimaker 3.

5.3 Equipment for dry-heat

An Espec brand temperature-humidity controlled test chamber was available for use for this thesis. A local calibration agent had calibrated the test chamber, and further machine specifications can be found from table 5.

Table 5. Specifications of the Espec PG-2KPH environmental test machine used for the simulated dry-heat treatment.

Model / Manufacturer	Espec PG-2KPH	-
Serial number	14014425	-
Manufacture date	2005	-
Temperature range	-40 - +140 ºC	± 0.3 ºC
Relative humidity range	Not required	-
Last calibration date	6/2019	By Kiwa Inspecta

The overview of the chamber is seen in Figure 24.

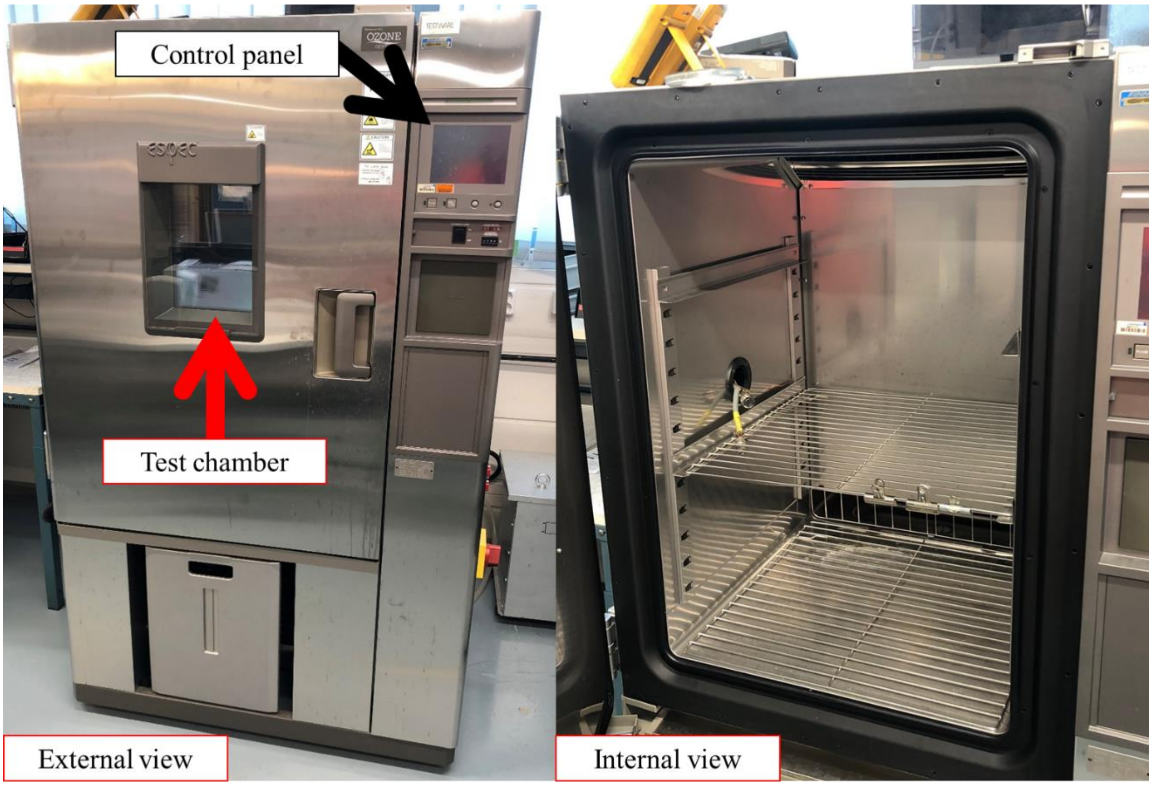

Figure 24. Environmental test machine Espec PG-2KPH external and internal view.

5.4 Equipment for tensile strength testing

The tensile test equipment specifications is presented in table 6.

Table 6. Specifications of the UTS systeme 100.20 tensile/compression test machine used for tensile testing.

Model / Manufacturer	UTS 100.20	
Software version	UTS Testsysteme V4.10	
Serial number	97112815	
Tensile test range	2-100 kN	
Tensile test resolution	5 N	
Tensile test accuracy	ISO 7500-1 Class 1	In 4kN range ± 0.37 % (14.8 N)

The tensile test system used was based on an old operating system and computer illustrated in Figure 25.

Figure 25. UTS systeme 100.20 tensile and compression testing machine setup.

5.5 Test specimen

A single test specimen geometry was selected according to the ISO 527-2 standard. The same test specimen design was used for the two test sets to obtain comparable results. The test set A was subjected to DH bioburden reduction and test set B was left as manufactured for control. The number of specimens required per test set limited the design variables to a minimum. Each test sets had ten specimens, of which five specimens were subjected to DH treatment. The minimum number of the specimen was specified in ISO 527-1 paragraph 7. Figure 26 represents the test specimen geometry.

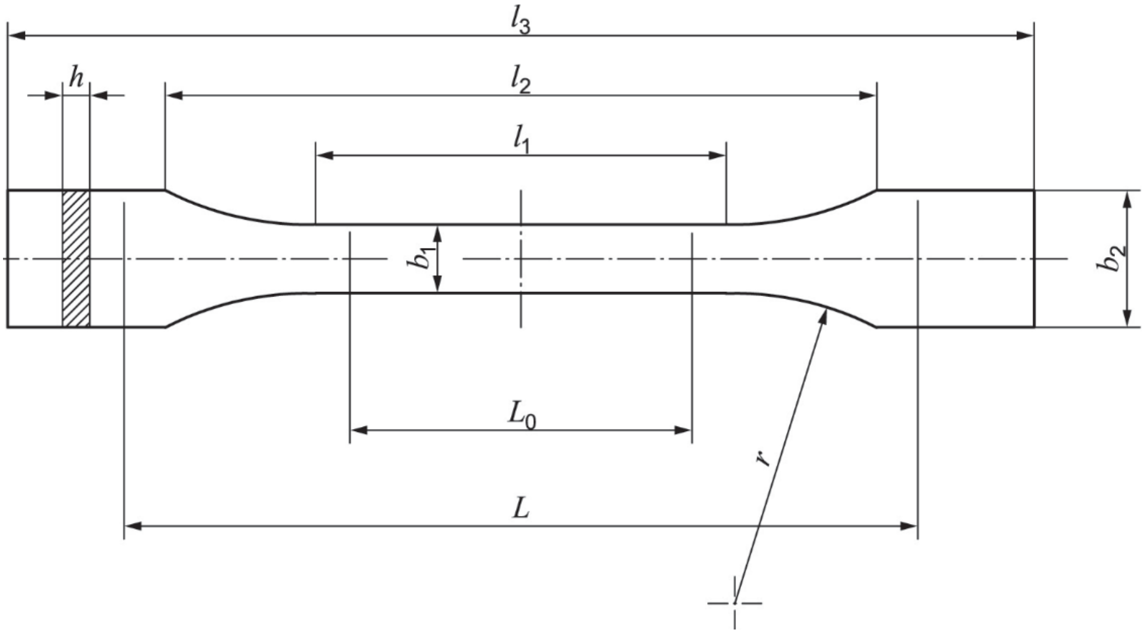

Figure 26. Test specimen geometry for plastic tensile test specimen according to ISO 527-2 for type 1A and 1B (Finnish Standards Association, 2012).

Multiple test specimen types are specified in the ISO 527-2, of which type 1A can be used for directly injection molded or compression molded specimens. The type 1B is described to be suitable for machined samples. This thesis has both machined and AM specimens, and therefore, it was chosen to select only one, type 1B. Limited data were available with similar experiments covering to types of manufacturing techniques in one. Previously conducted studies on AM tensile strength have presented type 1B as the selected type (Gunaydin, 2018). The dimension specified in ISO 527-2 for type 1B is presented in table 7.

Table 7. Dimensions for type 1B test specimen as per ISO 527-2, all dimensions are in millimeters (Finnish Standards Association, 2012).

	Specimen type	**1A**	**1B**
l_3	Overall length	170	≥ 150
l_1	Length of narrow parallel-sided portion	80 ± 2	60.0 ± 0.5
r	Radius	24 ± 1	60.0 ± 0.5
l_2	Distance between broad parallel-sided portions	109.3 ± 3.2	108 ± 1.6
b_2	Width at ends	20.0 ± 0.2	
b_1	Width at narrow portion	10.0 ± 0.2	
h	Preferred thickness	75.0 ± 0.5	4.0 ± 0.2
L_0	Gauge length (preferred)	50.0 ± 0.5	50.0 ± 0.5
L	Initial distance between grips	115 ± 1	115 ± 1

Each manufactured specimen was labeled for traceability purposes as per table 8. Specimens labeled A, were subjected to the DH process.

Table 8. Test specimen identification, as-printed manufacturing method, and applied bioburden reduction by dry heat.

Test specimen	**Manufacturing method**	**Material**	**Applied bioburden reduction**
A1	AM	PC filament	DH @ + 125 ºC for 71h
A2	AM	PC filament	DH @ + 125 ºC for 71h
A3	AM	PC filament	DH @ + 125 ºC for 71h
A4	AM	PC filament	DH @ + 125 ºC for 71h
A5	AM	PC filament	DH @ + 125 ºC for 71h
A6	AM	PVDF-C filament	DH @ + 125 ºC for 71h
A7	Milling	PC sheet	DH @ + 125 ºC for 71h
A8	Milling	PC sheet	DH @ + 125 ºC for 71h
A9	Milling	PC sheet	DH @ + 125 ºC for 71h
A10	Milling	PC sheet	DH @ + 125 ºC for 71h
A11	Milling	PC sheet	DH @ + 125 ºC for 71h
B1	AM	PC filament	None
B2	AM	PC filament	None
B3	AM	PC filament	None
B4	AM	PC filament	None
B5	AM	PC filament	None
B6	Milling	PC sheet	None
B7	Milling	PC sheet	None
B8	Milling	PC sheet	None
B9	Milling	PC sheet	None
B10	Milling	PC sheet	None

The manufacturer reported temperature limits are presented in table 9.

Table 9. Fundamental temperature values are given by manufacturers (Arla Plast, 2014; Nile Polymers, 2018; Ultimaker, 2018).

Material	**Heat deflection [ºC]**	**Continuous use [ºC]**	**Glass transition [ºC]**	**Melting [ºC]**
PC-filament	-	110	112	-
PC-sheet	142	-	147	-
PVDF-C filament	51	-	-	137

The heat deflection is a standard term for specific deflection caused under specified stress at the indicated temperature. Manufacturers occasionally report maximum temperature values for the materials they manufacture, including continuous use and glass transition temperatures.

6 EXPERIMENTAL PROCEDURE

This section discusses the procedures applied to the test specimen. Figure 27 presents the steps applied in the experiment to assess the suitability of PC for DH.

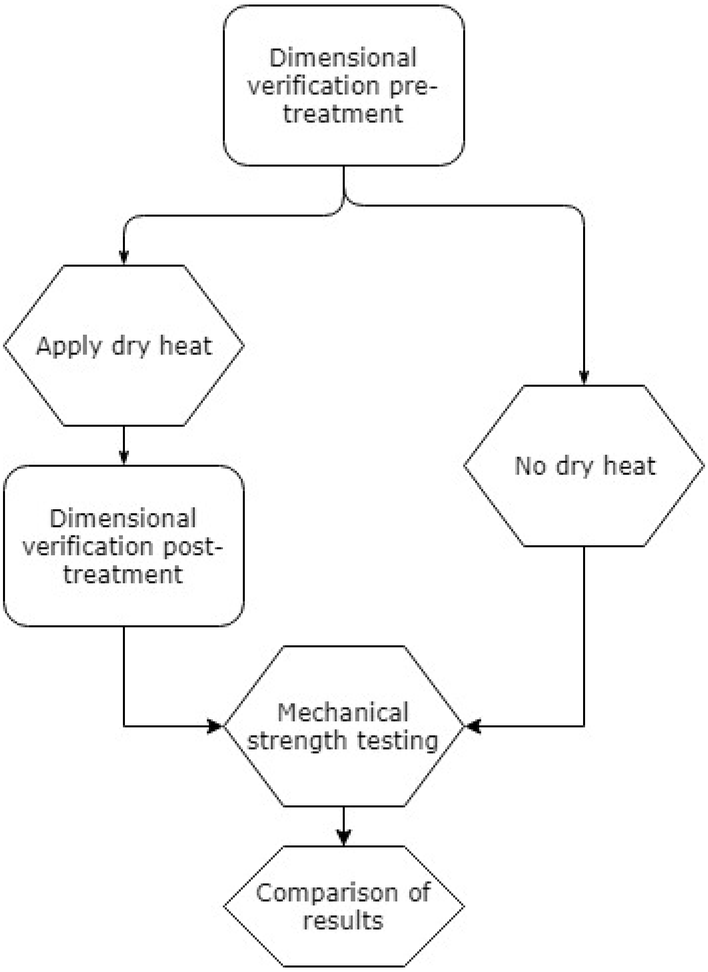

Figure 27. Experiment steps for each batch of test specimens for this thesis.

6.1 Manufacturing of test specimens with material extrusion and milling

Table 10 shows the printer settings used during the manufacturing of the ME PC test specimen. The manufacturing was performed at Maker3D Oy based in Helsinki.

Table 10. Print settings and data for PC AM test specimens, slicing software Cura 4.2. Wall thickness set to 15mm to enable nozzle movement straight on a narrow section.

Material selection	Ultimaker White PC
Printing temperature [ºC]	270
Build plate temperature [ºC]	110
Fan speed [%]	-
Layer height [mm]	0.15
Nozzle size / print core [mm]	0.80
Shell wall thickness [mm]	15.0
Infill density [%]	100
Total parts printed	11
Total material use [g]	108
Total material length [m]	14.2
Total material cost [€]	9.72
Total print time [h:mm]	8:37

The Ultimaker Cura-software was used to slice the specimen, as seen in Figure 28.

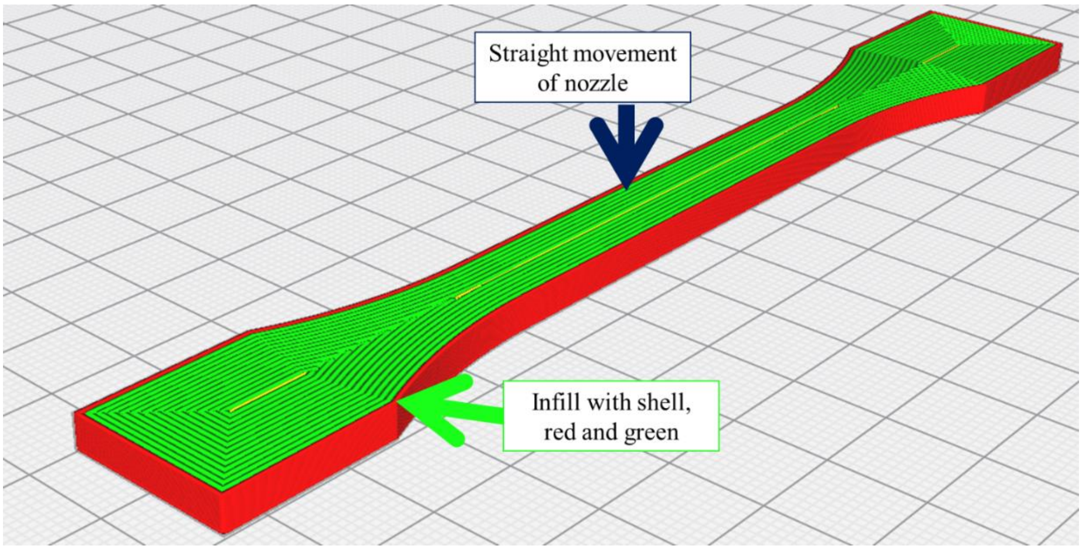

Figure 28. Preview of nozzle travel in Cura 4.2-software with single test specimen slice.

A close of the layers and nozzle travels can be seen from Figure 29.

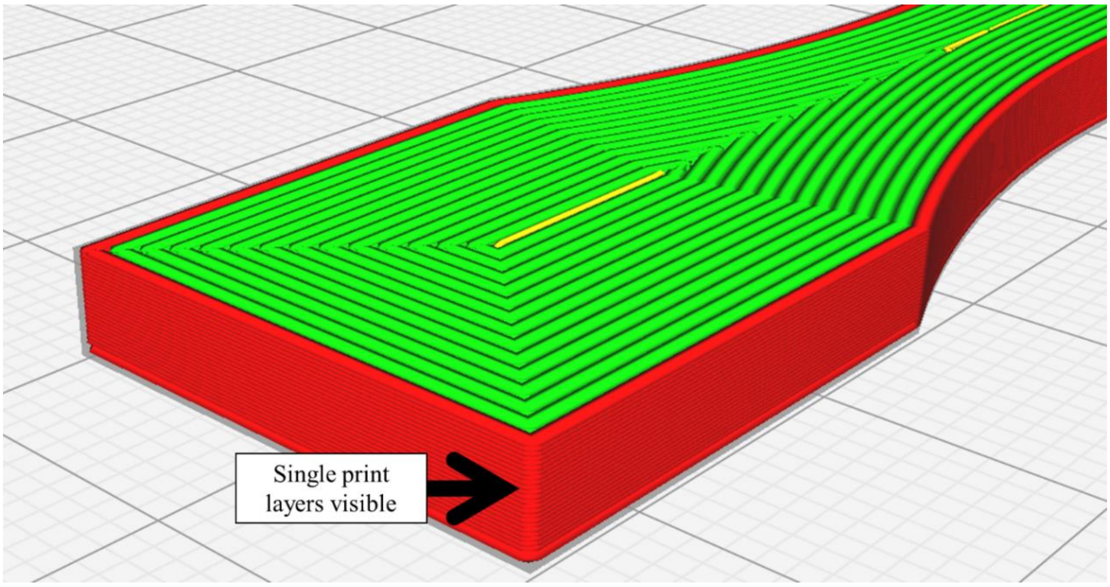

Figure 29. Single print layers, as per selected print settings, ready to be exported to the 3D-printer.

The single PVDF specimen was produced with table 11 print settings.

Table 11. Print settings and data for PVDF-C AM test specimen, slicing software Cura 4.2. Wall thickness set to 15mm to enable nozzle movement straight on a narrow section.

Material selection	Ultimaker White PC
Printing temperature [ºC]	200
Build plate temperature [ºC]	60
Fan speed [%]	100
Layer height [mm]	0.15
Nozzle size / print core [mm]	0.80
Shell wall thickness [mm]	15.0
Infill density [%]	100
Total parts printed	1
Total material use [g]	18
Total material length [m]	1.53
Total material cost [€]	5.57
Total print time [h:mm]	0:40

The Cura-software was a simple program used to manipulate the CAD-files to produce the AM samples by ME. The layout of the program and the setup of parameters can be seen in Figure 30.

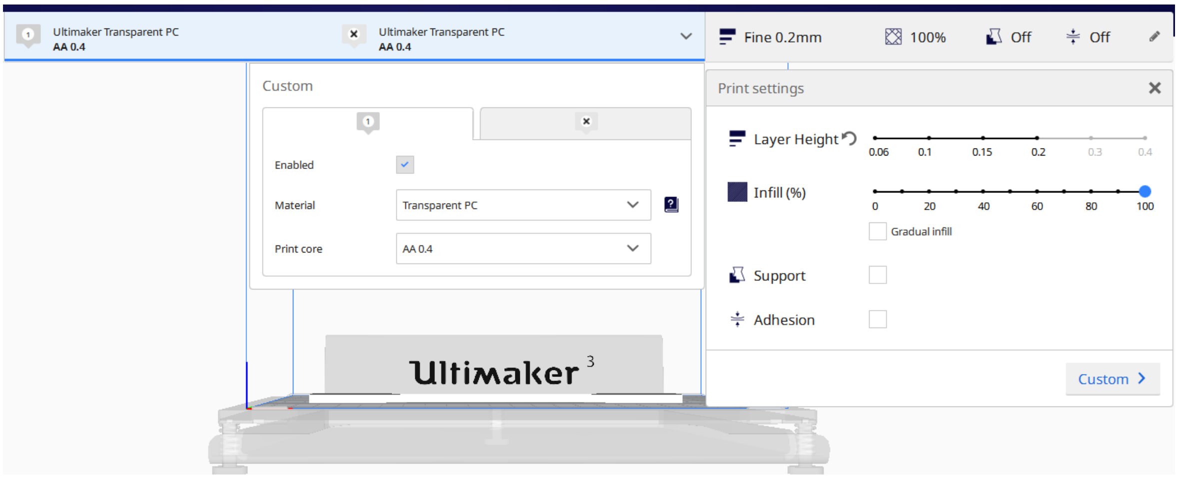

Figure 30. Setup of Cura-software with the selected machine, PC filament, layer height, infill according to software recommendation.

The milled samples were prepared with the Excitech milling machine using the parameters listed in table 12.

Table 12. Milling settings and tool description.

Tool diameter	5 mm
Tool material	High-speed steel
Tool rotating speed	16000 rpm
Tool feed rate	1500 mm/min

6.2 Measurement of test specimens

All test specimens were measured from locations seen in Figure 31 pre- and post-treatment to detect any deformation in the specimen.

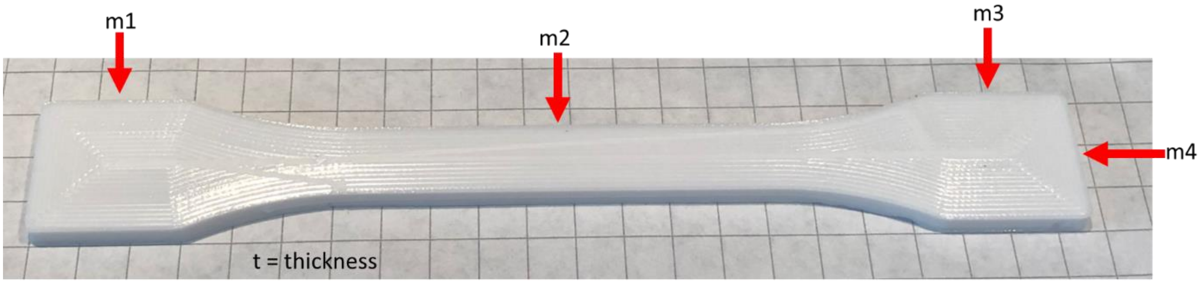

Figure 31. Measurement points used to verify dimensions with Vernier caliper. Photo of an actual test specimen. Measure points m_1 and m_3 are within 5 mm of the end of the specimen. The points m_2 and t are measured within 5 mm of the center point as per ISO 527:2012 9.2.

6.3 Measurement of tensile strength

Initial plans included to tensile test all specimens, both AM and sheet. Milled specimen were not tensile tested due to lack-of-time. One un-controlled specimen was tested for the sake of practice with the material. The un-controlled sheet specimen took nearly 30 minutes to test, due to testing speed of 5 mm/min and high elasticity of the sheet type PC specimen. This lengthy testing time was another reason to leave out the sheet specimens. The AM specimens provided a much shorter testing time as the material has a lower elongation factor.

The values for the tensile test process were gathered from relevant standards and are listed in table 13.

Table 13. Parameters and conditions during tensile testing.

Description	Value	Reference
Test speed	5 mm/min	ISO 527-1:2012, 5.1.2, table 1
Ambient temperature	22.6 ºC	ISO 527-1:2012, 8, 23 ± 2 ºC
Relative humidity	42 %	ISO 527-1:2012, 8, 50 ± 10 %
Extension meter	Not available	-
Test specification	ISO 527-2 / 1B / 5	ISO 527-2:2012, 11a

Finally, the test specimen was tightened one by one between the jaws of the test system, as seen in Figure 32, and the above parameters used to perform the testing.

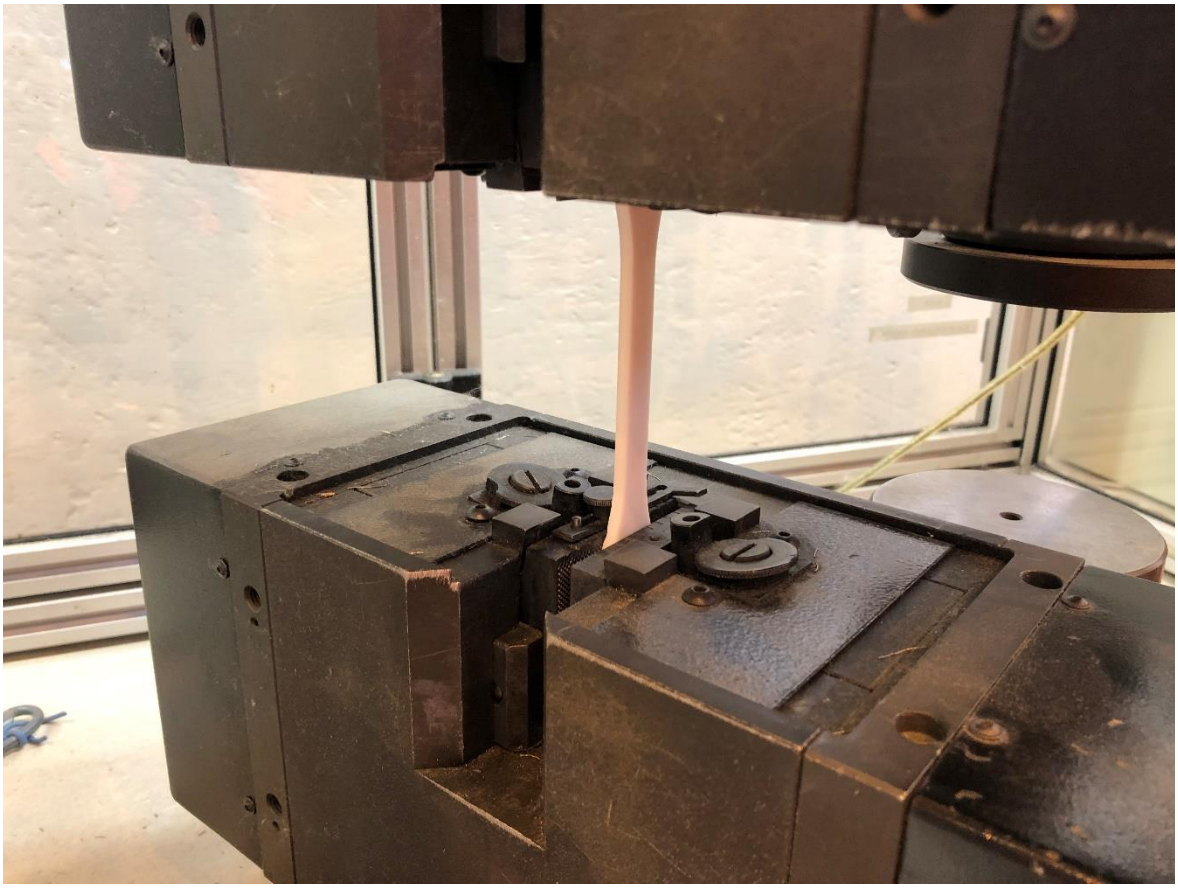

Figure 32. Test specimen mounted onto the tensile test system jaws by clamping.

6.4 Process for dry-heat

The requirements were found from ECSS-standards and provided a set of requirements to ensure sterilization of the flight hardware. The main requirement was driven by the bioburden reduction level, in this case, an order of five magnitude reduction.

Process temperature was selected to be +125 ºC and process time to 71 hours, with consideration of material properties. The equipment would need to reach these process requirements at a minimum. If the equipment would be used for actual flight hardware, the test chamber should be thoroughly cleaned with isopropanol and preferably a high-temperature cycle before bioburden reduction.

The main objective of the DH process was to apply elevated temperatures for this 71-hour uninterrupted period to reduce bioburden contaminants from the test specimens. Figure 33 graphically present the temperature variation over time used in the study, not to scale. Specimens were wiped with a lint-free cloth and 60/40-ratio of isopropanol/di-ionized water.

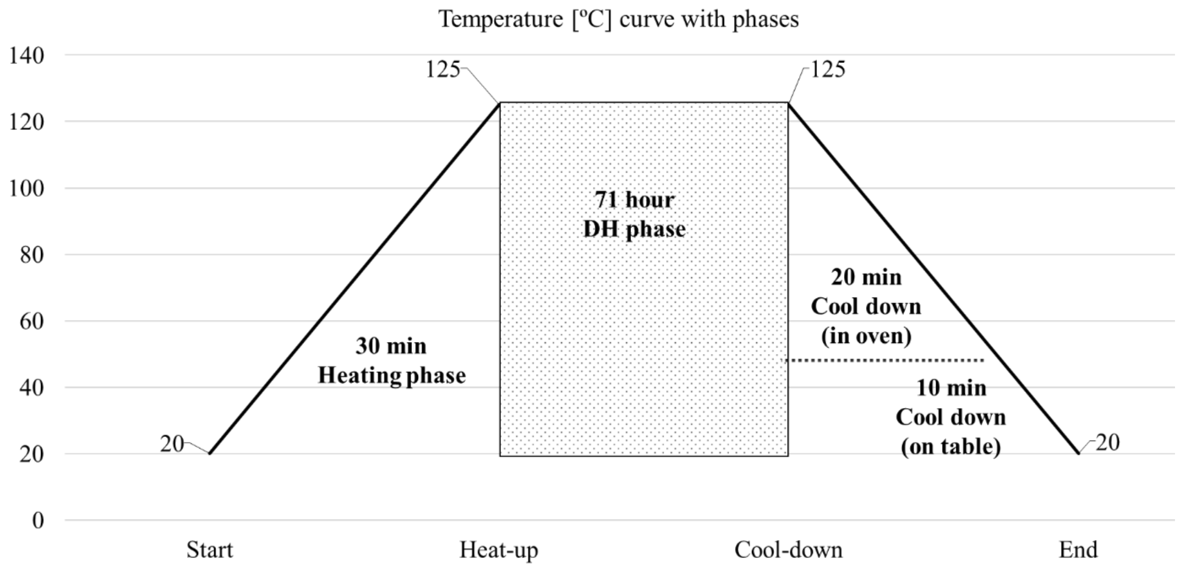

Figure 33. Temperature curve, cool down in the oven to 50 ºC.

Test specimen were laid on a rigid surface to prevent warping during heating and cooling of the DH process, identified specimen on the surface is presented in Figure 34.

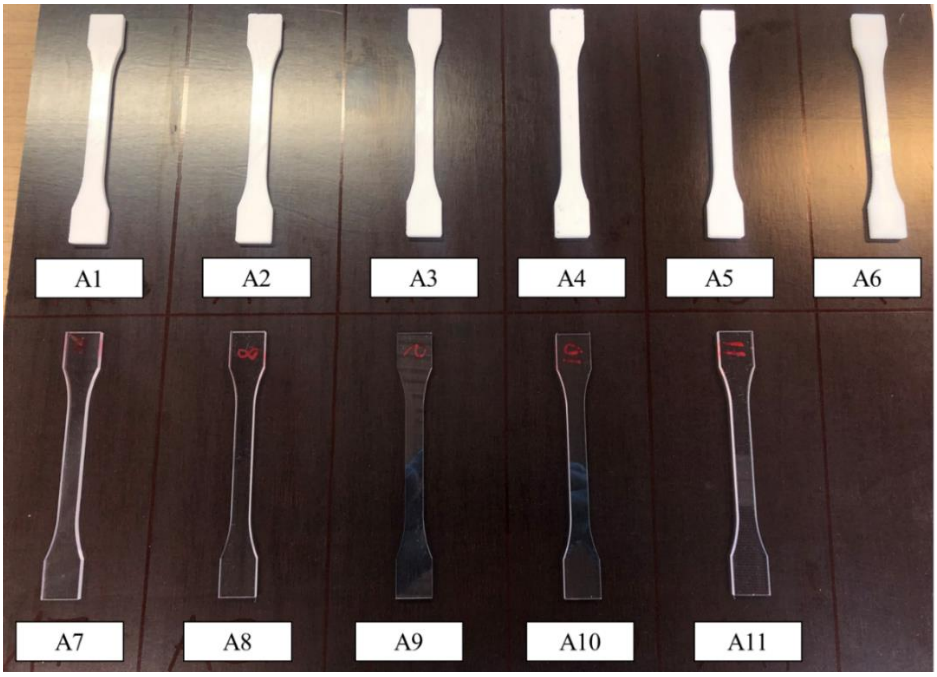

Figure 34. The test set A on rigid waterproof plywood pre-DH.

The DH-process was applied to the A1-A11 test specimens and then removed from the heated chamber after the cool-down. The specimens A7-A11 were not tensile tested later. After this, the specimens were inspected and measured similarly to pre-treatment.

7 RESULTS AND DISCUSSION

The results of the experimental portion are presented in this chapter. Applying the DH process on the AM test specimen assisted in confirming the suitability of the process and provide a look into the effects of heat on the test samples made of PC.

The experimental part was designed to provide a practical example and design suggestions for space-use AM parts. The manufacturing of the PC test specimens was completed by a sub-contractor, using a UM5 machine. Measures of the parts were taken after manufacturing to check the accuracy of the printing process and look for any defects. Figure 35 presents a single test specimen and a close-up of the post-manufacturing quality. Measurements of each specimen were taken pre- and post-DH and results are presented in Appendix I. The edges of the test specimens had some uneven surfaces, which caused measurement errors of ± 0.2 mm.

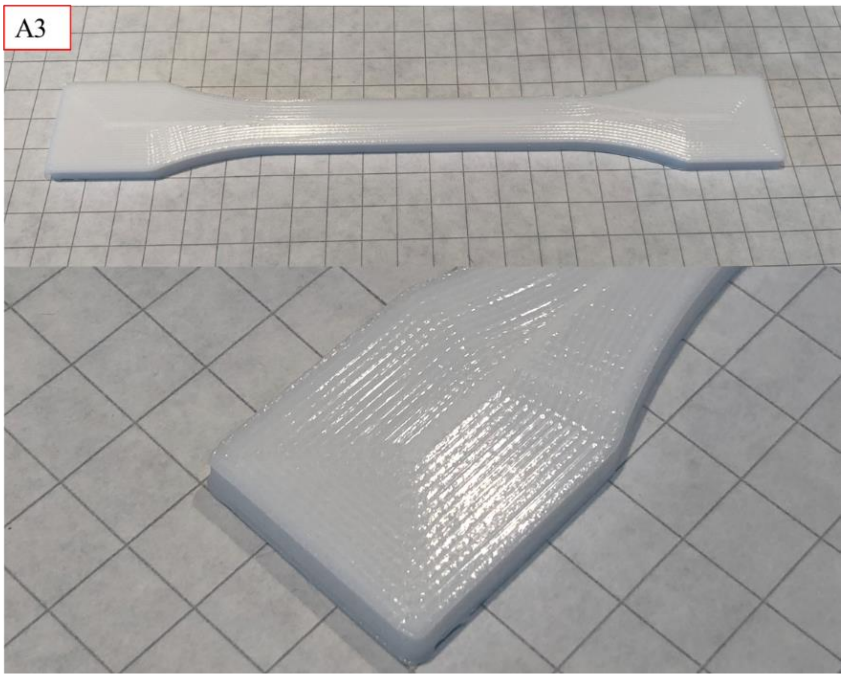

Figure 35. Test specimen A3 after printing, no visible defects, or discoloration visible. Measurements were taken and verified that none of the specimens were more than ±0.8 mm from the designed dimensions.

The specimen A3 represents the overall quality seen in all the test specimens. The nozzle travel paths were visible as with nearly all ME manufactured parts. Smoother surfaces and layer resolutions would have been achievable with other AM methods, but the machine prices would have differed from that of the used machine. The single PVDF test specimen A6 showed ruggedness on the top layer outer edge seen in Figure 36. The A6 specimen was confirmed to have a tensile strength of 29.4 MPa after a lengthy tensile test, which was due to the high elongation factor of PVDF. Further analysis of the A6 specimen was not performed, as it was not in the center point of this thesis.

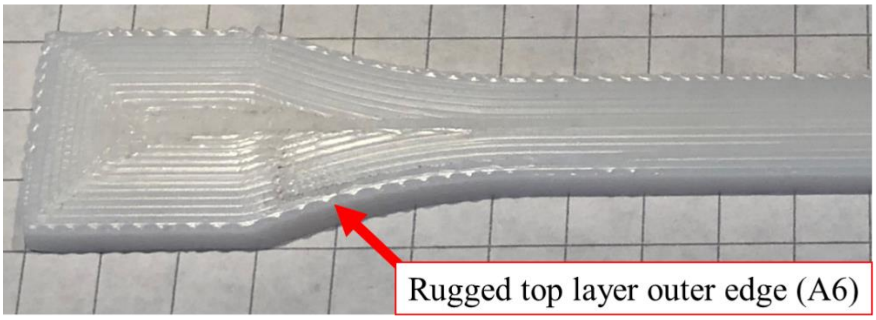

Figure 36. Test specimen A6 manufactured of PVDF showed some rugged texture, which could be felt by hand but did not affect the manual measurements.

Visual inspection confirmed that no discoloration or visible defects were present on the PC specimen. During measurements, it was noticed that the PC AM test specimens had shrunk in total length, on average, approximately 2.5 % or 3.9 mm. The average length of the test specimen pre- and post-treatment are presented in table 14. The other dimension, width, and thickness did not have such changes present. Detailed measurements and visual inspection results are summarized in Appendix I.

Table 14. The measurement result of length m_4 test result key figures, including average, standard deviation and peak stress. The first column includes all specimens prior to treatment. The second column includes only treated B-set specimens.

	Length [mm] test set A1-A5, B1-B5	**Length [mm], test set B1-B5**
Average	150.4	146.4
Standard deviation	0.264	0.948
Change post-treatment	-	-3.9

The length measurement results pre-treatment are presented in Figure 37.

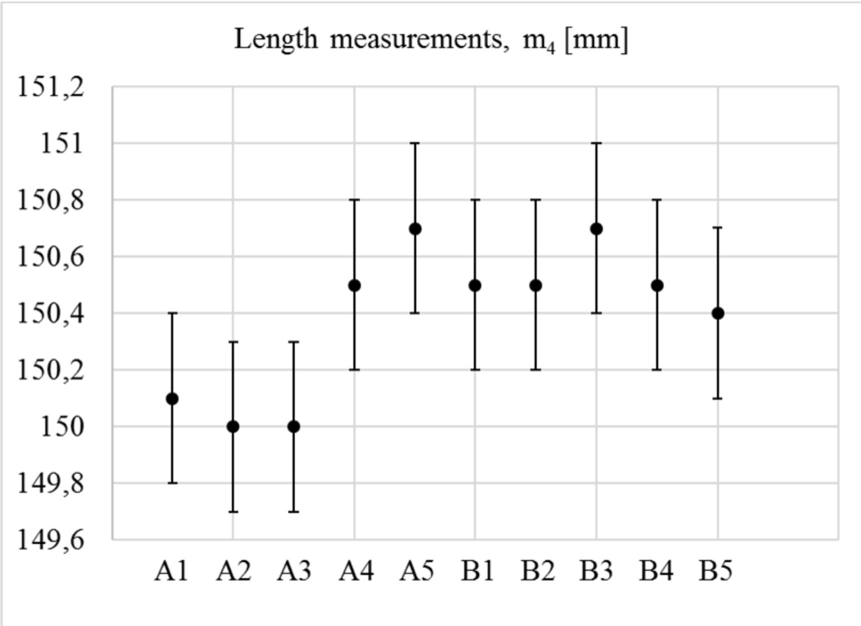

Figure 37. Test specimen length measurement results without DH treatment. Measurement accuracy set to 0.2 %.

It was evident that nearly all samples were measured to be larger than the designed length of 150 mm. The maximum lengths were seen with A5 and B3 specimen, but when compared to the full length of the specimen presented a difference of merely 0.5 % from designed. The ISO 527-2 specified only the minimum length of the test specimen, so the inaccuracy represented the ME machines capability in this thesis. The other tolerances presented in ISO 527-2 were not met on the widths of the test samples, as the given tolerance was only ±0.2 mm and was exceeded by many specimens. The thicknesses of all samples were within the tolerance of the standard.

The B-set of test specimen was subjected to DH and measurements are presented in Figure 38.

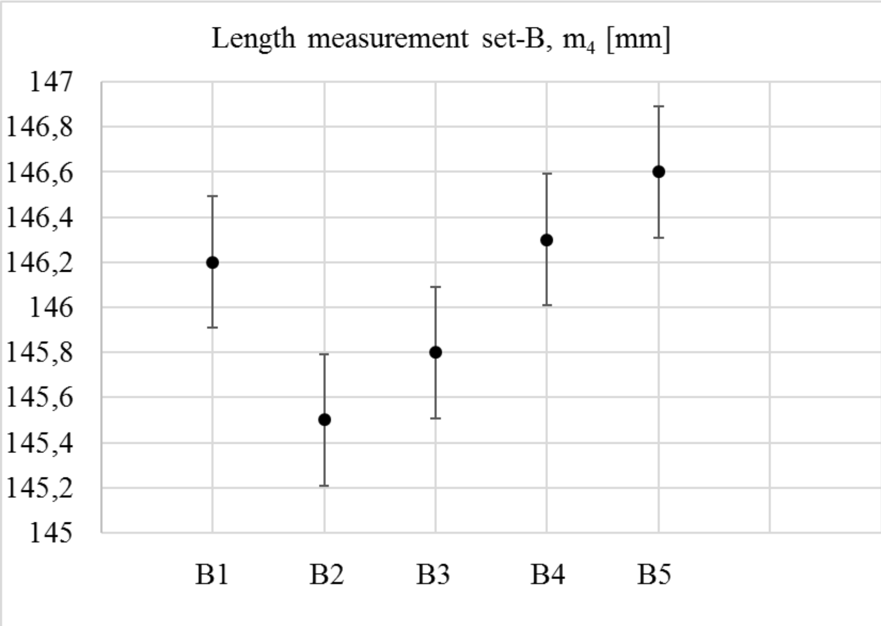

Figure 38. The test set B length measurements post-DH. Measurement accuracy set to 0.2 %.

The obtained tensile strengths, along with maximum break forces, are presented in table 14.

Table 14. Tensile test result for AM specimens. Tensile strength is based on the cross-section area of 40mm^2.

Manufacturing	**Specimen**	**Material**	**Break force [N] ± 14.80 N**	**Tensile strength, at break [MPa]**
AM	A1	PC	2621	65.53
AM	A2	PC	2669	66.73
AM	A3	PC	2678	66.95
AM	A4	PC	2617	65.43
AM	A5	PC	2659	66.48
AM	A6	PVDF-C	1175	29.38
AM	P1	PC	2641	66.03
AM	B1	PC	2645	66.13
AM	B2	PC	2650	66.25
AM	B3	PC	2624	65.60
AM	B4	PC	2643	66.08
AM	B5	PC	2642	66.05

The maximum break forces with 0.37 % force measurement inaccuracy is presented in Figure 39.

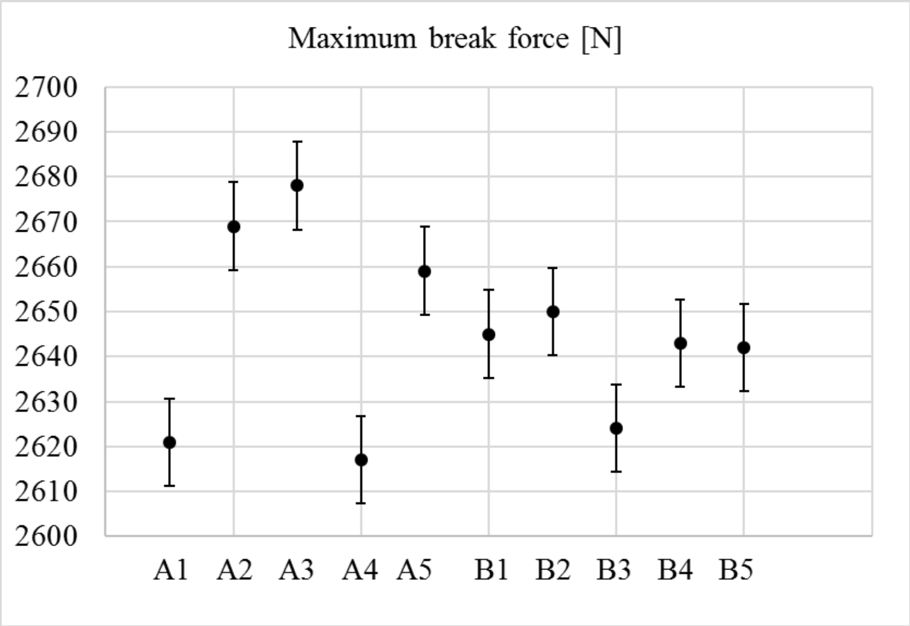

Figure 39. Maximum break forces of the AM test specimen with machine-specific force measurement tolerance.

The tensile strengths at break, including inaccuracies, are presented in Figure 40.

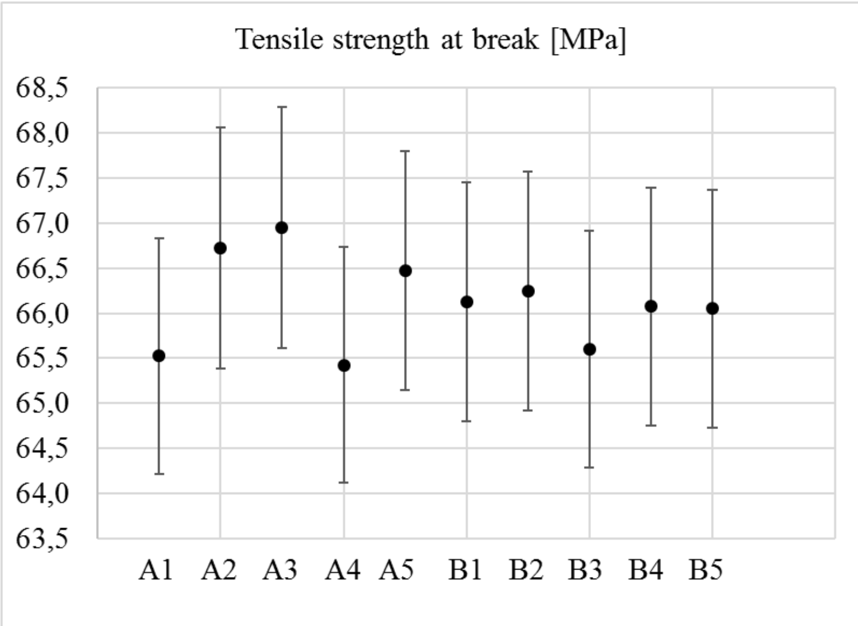

Figure 40. Tensile strength at break, with 2.00 % inaccuracy calculated from the force measurement inaccuracy 0.37% and thickness and width deviations compared to design value, then rounded from the second decimal place. Calculated with a 40 mm^2 cross-section.

Key figures of the tensile test results are presented in table 15, derived from the values presented in table 14.

Table 15. Tensile test result key figures, including average, standard deviation and peak stress.

	Value [MPa], test set A1-A5	**Value [MPa], test set B1-B5**
Average	66.2	66.0
Standard deviation	0.70	0.25
Peak Stress	67.0	66.3

The computerized tensile test system was not able to print out clear values of strain as no external extensometer was installed and old software. An approximate value is presented in Figure 41, which is based on the value calculated by the software.

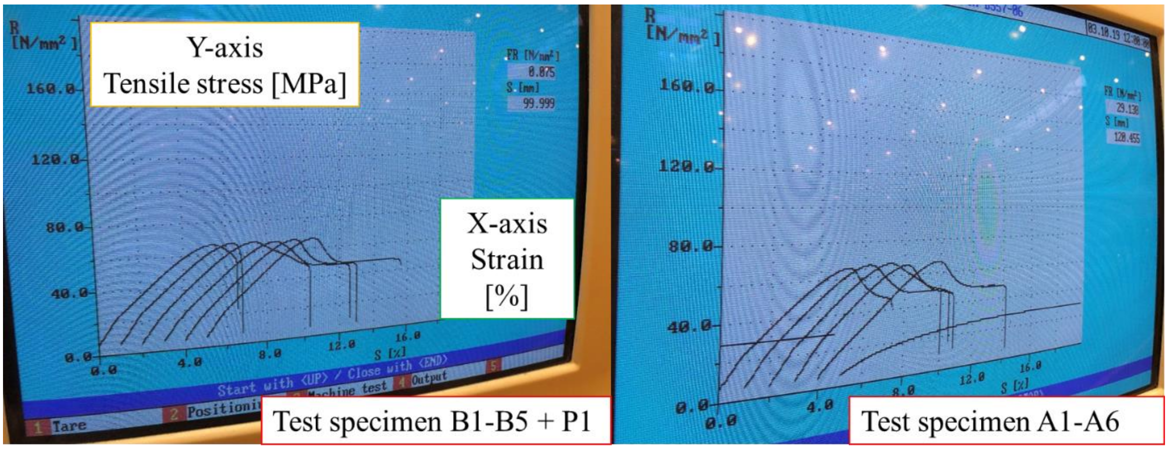

Figure 41. Tensile test results in graphical format captured from the computer screen, no accurate strain values are available only approximations made by the test system. Results start from left to right in ascending order.

The specimen all broke with similar tear patterns visible in Figure 42. Nearly all test specimens broke near the midpoint of the specimen, but B2 broke slightly offset from the midpoint while presenting similar tensile strength.

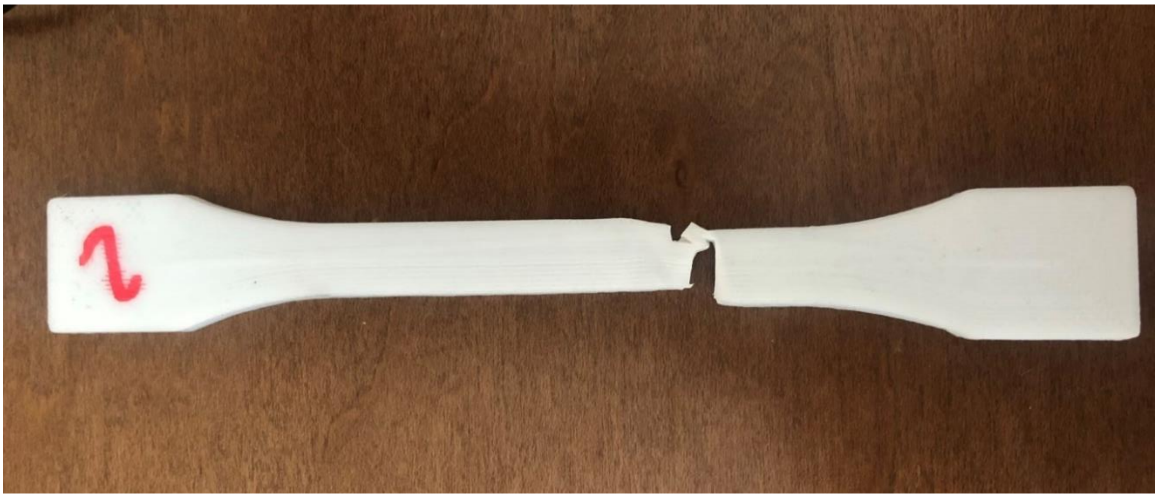

Figure 42. Test specimen B2 after tensile testing. The tear of the sample occurred slightly offset from the midpoint, but the tensile strength was still in line with other results.

A simplified flow chart was created, Figure 43, to illustrate the bioburden control phases found during the literature review. One of the goals of this thesis was to create awareness of the main steps in bioburden reduction to assist agile space companies to better prepare.

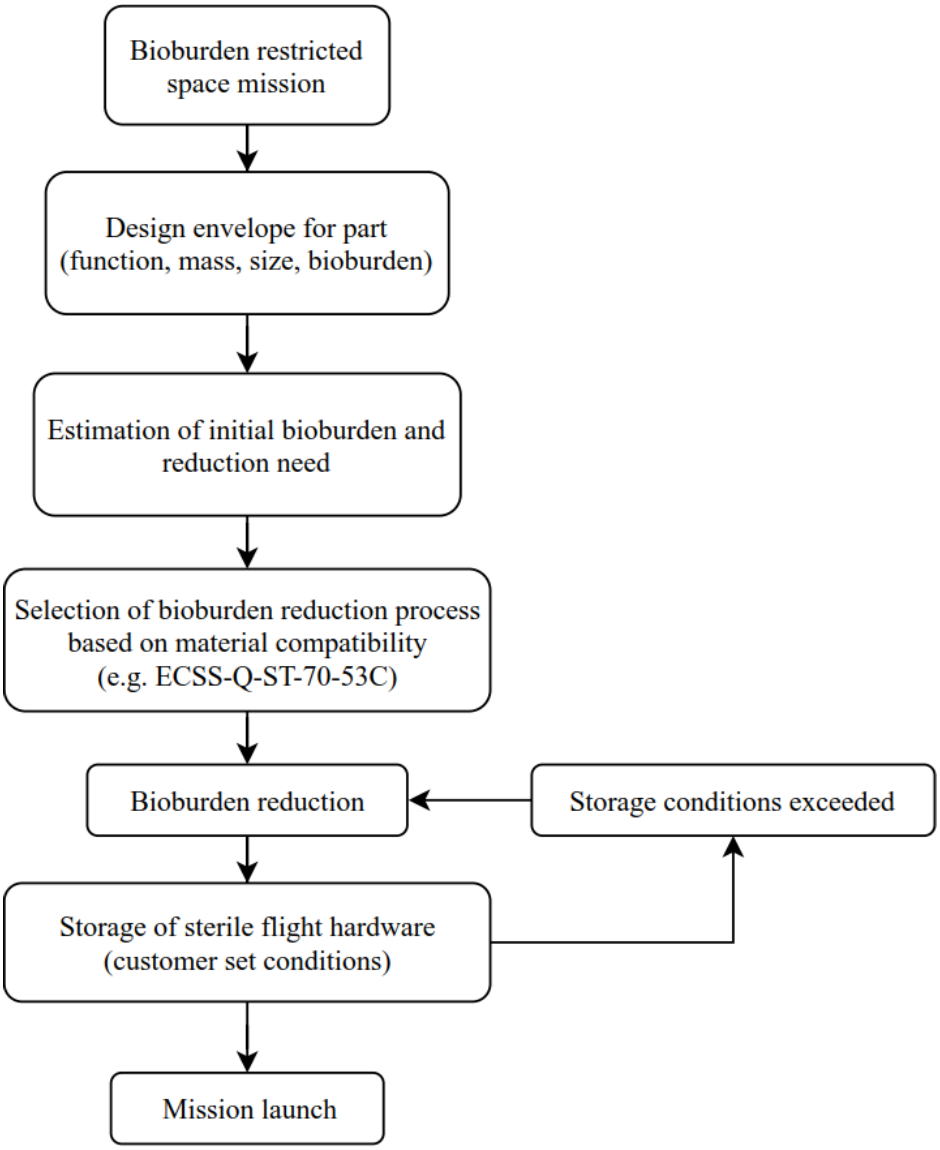

Figure 43. Bioburden process from design to mission launch, simplified process diagram.

The process diagram described in Figure 43 was derived from industry standards and focused on bioburden reduction methods applicable to a pre-mission period. The initial requirements would have come from the customer preparing the specific mission, by a written agreement. The primary responsibility of the supplier would have been the application and reporting of the bioburden activities and possible plans for possible mission delays, should the parts have not been integrated into the entire spacecraft assembly already. The requirements have focused on the traceability of processes and equipment expected from the supplier (ESA Requirements and Standards Division, 2008b).

8 CONCLUSIONS

ME is a widely available AM process, which can produce parts made from materials suitable for the space industry. The restricted number of available materials is seen when comparing the number of available polymeric materials with those suitable for space. The AM machine requirements, set by the material, vary with different materials. The mission profile discussed in this thesis further added requirements to material characteristics, brought by bioburden control. s

The goal of this thesis was first to study requirements for the specified mission and present a practical example of material suitability with the DH bioburden control process. Bioburden requirements were gathered and applied in practice. Half of the AM test specimen were cycled in the DH process, and all visible effects were documented, as well as dimensional changes and tensile strength variations to the control group.

The main research questions of this thesis were:

- How to assist agile space companies in understanding bioburden control in an additive manufacturing framework by adding awareness and providing a practical experiment?
- Can desktop size 3D-printer materials withstand dry heat bioburden reduction in an environmental chamber?

By presenting the flow chart for bioburden control and tensile test results, it was believed that both research questions were answered. The complex nature of each step of the bioburden control process flow requires further study from companies on current standards to understand how to achieve required bioburden control fully. It is up to the missions PP responsible for defining and determining what acceptable bioburden levels are and the responsibility of the supplier company to implement bioburden control measures and report the achieved bioburden level to the customer.

The main requirements for bioburden control were defined in the PP policy and further referenced in agency and industry standards. Clear bacterial limitations were not defined for the mission type-specific to Enceladus, but the risk of accidental contamination needs to be within set limits. It was chosen to apply a high reduction process to better demonstrate preparedness for possible missions to Enceladus with polymeric AM materials on-board.

The development of the PP policy would have been preferred towards defining bacterial limitations for objects of interest accurately. Though there remained the open question of assessing specific bacterial forms that would be of highest concern on any specific missions. The criticism seemed to be well-argued and had solid examples as well as ways to move forward. It was valuable to see that the scientific community was not suppressed by the current conditions but has rather strived to figure out ways to move forward. The changes in PP policy would have to be carefully considered in order to prevent accidental contamination, jeopardizing future scientific discoveries. A balance needs to be found between the rate of scientific discovery and related risks within a mission.

It was demonstrated that a commercially purchased AM material, PC, could be subjected to bioburden reduction using DH. Comparing the tensile test results with specimens that were not subjected to DH, revealed that the tensile strength was not affected during the DH at +125 ºC for 71 hours. The only significant changes noticed with the DH test specimen when measuring was the shortening of the test specimen. It was determined that the specimens did not meet the ISO 527-2 standard in terms of width, which would require design modifications in the further tensile tests with similar specimens.

This represented the limitations of using commercial ME machines for producing higher accuracy parts or test specimens. A single test specimen would have been beneficial to manufacture prior to producing the entire batch, to reveal such inaccuracies and to be appropriately iterated to better comply with standards. This was also a lesson learned that the AM design could have been iterated rapidly and continued forward with the changes implemented into production. Therefore, it was a valuable lesson to understand that designs do need iterative design changes or possibly post-manufacturing to meet specifications. The preferred way to proceed would have been to alter the design to avoid unnecessary post-manufacturing tasks with traditional methods.

The standard tensile test specimen represented apart with a high length to width ratio and has limited applicability with other geometries, extraordinarily complex AM parts that are often produced due to the advantages of AM. Though it is time-consuming, it might be beneficial to produce prototypes to be subjected to DH or other bioburden reduction processes and verify the actual changes in dimensions of the part. Provided previous tests have not been performed on mechanical changes on the specific material, tensile strength, or others, it might be beneficial to produce some standard test specimen to verify such changes in case of doubt.

It was encouraging to discover that with minor effort, AM parts could be subjected to a treatment generally not applied to AM parts. The hypothetical mission was a starting point to what needs to be understood in order to send polymeric AM parts to Enceladus. It was clear there remain challenges with using polymers in space, especially how to verify outgassing values with reasonable effort in agile space projects. Additionally, materials have been evolving rapidly, and new mixtures of filaments have been commercialized. It was unclear to what extent would the changing material base have needed testing in order to satisfy agile space project demands, even on a space agency level. The future will show how the requirements will be satisfied.

One thing became clear, space exploration is about to change in many ways, and it is only a matter of time when AM will become the industry-standard method of manufacturing multi-function, multi-material, and complex parts. The embedded need to explore lives in all of us and only we can make it possible by continuing efforts together.

9 FUTURE STUDIES

Here are the thoughts raised during the writing of this thesis, on possible research topics for future studies:

- Implementation of storage requirements for sterile flight hardware and possible issues with mission delays.
- How to determine the survivability of risk bacteria, for life, on a specific mission type?
- Cost-efficient ways to perform CVCM and TML outgassing testing, with current or improved standards.
- How to determine bacterial content before bioburden control, based on standards and through practical examples.
- Combining bioburden reduction methods to achieve high-reduction, considerations, and available combinations.

LIST OF REFERENCES

Arla Plast (2014) 'MAKROCLEAR Data Sheet'.

ASTM International and ISO (2015) 'ISO / ASTM 52900 Additive manufacturing — General principles — Requirements for purchased AM parts'. ASTM & ISO.

Booth, J. W., Alperovich, J., Chawla, P., Ma, J., Reid T. N. and Ramani, K. (2017) 'The Design for Additive Manufacturing Worksheet', *Journal of Mechanical Design*, 139(October), pp. 1009041–1009049. doi: 10.1115/1.4037251.

Boschetto, A., Bottini, L., Eugeni, M., Cardini, V., Nisi, G. G., Veniali, F. and Gaudenzi, P. (2019) 'Selective Laser Melting of a 1U CubeSat structure. Design for Additive Manufacturing and assembly', *Acta Astronautica*. Elsevier Ltd, 159(January), pp. 377–384. doi: 10.1016/j.actaastro.2019.03.041.

Chua, C. K., Wong, C. H. and Yeong, W. Y. (2017) *Standards, Quality Control, and Measurement Sciences in 3D Printing and Additive Manufacturing*. Elsevier.

ESA (2001) *ESMAT database: PVDF outgassing data report number Estec/520*. Available at: http://esmat.esa.int/materialframe.html (Accessed: 9 August 2019).

ESA (2013) *ECSS-Q-ST-70-56C Space product assurance Vapour phase bioburden reduction*.

ESA Requirements and Standards Division (2008a) 'ECSS-Q-ST-70-53C Space product assurance: Materials and hardware compatibility tests for sterilization processes'. Noordwijk, The Netherlands: ESA Requirements and Standards Division.

ESA Requirements and Standards Division (2008b) 'ECSS-Q-ST-70-55C: Space product assurance Microbial examination of flight hardware and cleanrooms'. Noordwijk, The Netherlands: ESA Requirements and Standards Division.

ESA Requirements and Standards Division (2013) *ECSS-Q-ST-70-57C Space product assurance Dry heat bioburden reduction for flight hardware*.

Fairén, A. G., Schluze-Makuch, D., Whyte, L., Parro, V., Pavlov, A., Gómez-Elvira, J., Azua-Bustos, A., Fink, W. and Baker, V. (2019) 'Planetary Protection and the astrobiological exploration of Mars: Proactive steps in moving forward', *Advances in Space Research*, 63(5), pp. 1491–1497. doi: 10.1016/j.asr.2019.01.011.

Feynman, R. (1955) 'The Value of Science', *Engineering and Science*, XIX, pp. 13–15.

Finnish Standards Association (2012) 'EN ISO 527-2 : 2012 Plastics . Determination of tensile properties . Part 2 : Test conditions for moulding and extrusion plastics'. Helsinki, Finland: International Organization for Standardization.

Fortescue, P., Swinder, G. and Stark, J. (2011) *Spacecraft Systems Engineering*. 4th edn. Chichester, West Sussex: John Wiley & Sons, Ltd.

Fu, W., Haberland, C., Klapdor, E. V., Rule, D. and Piegert, S. (2018) 'Streamlined frameworks for advancing metal based additive manufacturing technologies', *Journal of the Global Power and Propulsion Society*, 2(January). doi: 10.22261/jgpps.qjls4l.

Gaudenzi, P., Atek, S., Cardini, V., Eugeni, M., Nisi, G. G., Lampani, L., Pasquali, M. and Pollice, L. (2018) 'Revisiting the configuration of small satellites structures in the framework of 3D Additive Manufacturing', *Acta Astronautica*, 146, pp. 249–258. doi: 10.1016/j.actaastro.2018.01.036.

Gibson, I., Rosen, D. W. and Stucker, B. (2010) *Additive Manufacturing Technologies, CIRP Encyclopedia of Production Engineering*. doi: 10.1007/978-1-4419-1120-9.

Gordon, J. A., Novotny, D. R., Francis, M. H., Wittman, R. C., Butler, M. L., Curtin, A. E., Guerrieri, J. R., Periasamy, L. and Gasiewski A. J. (2017) 'An All-Metal, 3-D-Printed CubeSat Feed Horn', (april), pp. 2–8.

Grossman, E. and Gouzman, I. (2003) 'Space environment effects on polymers in low earth orbit', *Nuclear Instruments and Methods in Physics Research, Section B: Beam Interactions with Materials and Atoms,* 208(1–4), pp. 48–57. doi: 10.1016/S0168-583X(03)00640-2.

Gunaydin, K. (2018) 'The Effect of Layer Thickness to the Tensile Stress : Experimental Studies The effect of layer thickness to the tensile stress', (April).

Hällgren, S., Pejryd, L. and Ekengren, J. (2016) '(Re)Design for Additive Manufacturing', *Procedia CIRP*. The Author(s), 50, pp. 246–251. doi: 10.1016/j.procir.2016.04.150.

Halliday, D., Resnick, R. and Walker, J. (2011) *Fundamentals of Physics 9th Edition*.

Hecthel, D. K. (2014) *Design Considerations for the Use of Plastic Materials in Cryogenic Environments*. Curbell Plastics Inc.

Hopkinson, N. and Dickens, P. (2003) 'Analysis of rapid manufacturing - Using layer manufacturing processes for production', Proceedings of the Institution of Mechanical Engineers, Part C: Journal of Mechanical Engineering Science, 217(1), pp. 31–40. doi: 10.1243/095440603762554596.

Imken, T. Sherwood, B., Elliot, J., Frick, A., McCoy, K., Oh, D., Kahn, P., Karapetian, A., Polit-Casillas, R., Cable, M., Lunine, J., Kempf, S., Southworth, B., Tucker, S. and Waite, J. H. (2016) 'Sylph – A SmallSat Probe Concept Engineered to Answer Europa ' s Big Question', in *30th Annual AIAA/USU Conference on Small Satellites*.

Intamsys (2019) 'FUNMAT HT 3D PRINTER User manual'.

Kirchheim, A., Dennig, H.-J. and Zumofen, L. (2017) 'Why Education and Training in the Field of Additive Manufacturing is a Necessity: The Right Way to Teach Students and Professionals', in *Industrializing Additive Manufacturing - Proceedings of Additive Manufacturing in Products and Applications - AMPA2017*. Springer International Publishing. doi: 10.1007/978-3-319-66866-6.

Klesh, A. and Krajewski, J. (2018) ‘MarCO: Mars Cube One – Lessons Learned from Readying the First Interplanetary Cubesats for Flight’, in *49th Lunar and Planetary Science Conference 2018*, pp. 1134–1140.

Kminek, G., Conley, C. Hipkin, V. and Yano, H. (2017) ‘COSPAR ’ s Planetary Protection Policy’. COSPAR. doi: 10.1016/j.srt.2017.11.010.

Kminek, G. (2018) ‘COSPAR Planetary Protection Policy’, in *69th International Astronautical Congress*. Bremen, Germany: COSPAR.

Kumar, L. J. and Nair, C. G. K. (2017) *Current Trends of Additive Manufacturing in the Aerospace Industry*, *Advances in Manufacturing & Additive 3D Printing Technologies*. Edited by D. I. Wimpenny, P. M. Pandey, and L. Jyothish Kumar. Springer Nature. doi: 10.1007/978-981-10-0812-2_4.

Lyke, J. C. (2012) ‘Plug-and-Play Satellites’, *IEEE Spectrum*, pp. 36–42.

Madry, S., Martinez, P. and Laufer, R. (2018) *Innovative Design, Manufacturing and Testing of Small Satellites*, *Innovative Design, Manufacturing and Testing of Small Satellites*. Chichester, UK: Spinger Praxis Books. doi: 10.1007/978-3-319-75094-1.

Meltzer, M. (2011) *When Biospheres Collide: A History of NASA´s Planetary Protection Programs*. 1st edn. NASA.

Mitchell, K. L., Hodyss, R., Choukroun, M., Molaro, J. and Le Gall, A. (2018) ‘ENCELADUS’ BRILLIANT SURFACE 2: RATIONALIZING CASSINI RADAR AND OPTICAL REMOTE SENSING’, in *49th Lunar and Planetary Science Conference 2018*. Houston, Texas, pp. 1–2.

Mladenić, D., Brank, J. and Grobelnik, M. (2014) *CubeSat Design Specification*. 12th edn. San Louis Obispo: California Polytechnic State University. doi: 10.1007/978-1-4899-7687-1_75.

Morretton, E., Vignat, F., Pourroy, F. and Marin, P. (2019) ‘Impacts of the settings in a design for additive manufacturing process based on topological optimization’, *International Journal on Interactive Design and Manufacturing (IJIDeM)*. Springer Paris, 13(1), pp. 295–308. doi: 10.1007/s12008-018-00524-9.

Muraca, R. F. and Whittick, J. S. (1967) *Polymers for spacecraft applications*. Menlo Park, California.

Nile Polymers (2005) ‘Chemical Resistance Chart PVDF’, *Glass*, pp. 1889–900. doi: 10.1101/gr.327702.

Nile Polymers (2018) ‘Fluorinar-H ™ Kynar ® PVDF Filament’, pp. 1–6.

Pang, K. D. Voge, C. C., Rhoads, J. W. and Ajello, J. M. (1981) ‘E RING OF SATURN AND SATELLITE ENCELADUS.’, *Journal of Geophysical Research*, 89(B11), pp. 9459–9470. doi: 10.1029/JB089iB11p09459.

Park, S., Jeon, H., Kim, H., Shin, S., Choy, S., Hwang, D. S., Koo, J. M., Jegal, J., Hwan, S. Y., Park, J. and Oh, D. X. (2019) 'Sustainable and recyclable super engineering thermoplastic from biorenewable monomer', *Nature Communications*. Springer US, 10(1), pp. 1–11. doi: 10.1038/s41467-019-10582-6.

Poli, C. (2001) *Design for Manufacturing - A Structured Approach*. First. Elsevier.

Porco, C. C., Helfenstein, P., Thomas, P. C., Ingersoll, A. P., Wisdom, J., West, R., Neukum, G., Denk, T., Wagner, R., Roatsch, T., Kieffer, S., Turtle, E., McEwen, A., Johnson, T. V., Rathbun, J., Veverka, J., Wilson, D., Perry, J., Spitale, J., Brahic, A., Burns, J. A., DelGenio, A. D., Dones, L., Murray, C. D. and Squyres, S. (2006) 'Cassini Observes the Active South Pole of Enceladus', *Science*, 311(March), pp. 1393–1401. doi: 10.1126/science.1123013.

Porco, C. C., Dones, L. and Mitchell, C. (2017) 'Could It Be Snowing Microbes on Enceladus? Assessing Conditions in Its Plume and Implications for Future Missions', *Astrobiology*, 17(9), pp. 876–901. doi: 10.1089/ast.2017.1665.

Praks, J., Kestilä, A., Tikka, T., Leppinen, H., Khurshid, O. and Hallikainen, M. (2015) 'AALTO-1 earth observation cubesat mission - Educational outcomes', *International Geoscience and Remote Sensing Symposium (IGARSS)*, 2015-Novem, pp. 1340–1343. doi: 10.1109/IGARSS.2015.7326023.

Prantzos, N. (2013) 'A joint analysis of the Drake equation and the Fermi paradox', *International Journal ofAstrobiology*, 12(3), pp. 246–253. doi: 10.1017/S1473550413000037.

Reh, K., Lunine, J. I., Cable, M. L., Spilker, L., Waite, J. H., Postberg, Frank and Clark, K. (2016) 'Enceladus Life Finder: The search for life in a habitable Moon', in *IEEE Aerospace Conference Proceedings*. IEEE, pp. 1–8. doi: 10.1109/AERO.2016.7500813.

Singh, D., Singh, R. and Boparai, K. S. (2018) 'Development and surface improvement of FDM pattern based investment casting of biomedical implants: A state of art review', *Journal of Manufacturing Processes*, 31, pp. 80–95. doi: 10.1016/j.jmapro.2017.10.026.

Smith, B. A., Soderblom, L., Batson, R., Bridges, P., Inge, J., Masursky, H., Shoemaker, E., Beebe, R., Boyce, J., Briggs, G., Bunker, A., Collins, S. A., Hansen, C. J., Johnson, T. V., Mitchell J. L., Terrile, R. J., Cook II, A. F., Cuzzi, J., Pollack, J. B., Danielson, G. E., Ingersoll, A. P., Davies, M. E., Hunt, G. E., Morrison, D., Owen, T., Sagan, C., Veverka, J., Strom, R. and Suomi, V. E. (1982) 'A New Look at the Saturn System: The Voyager 2 Images', *Science*, 215(4532), pp. 504–537. doi: 10.1126/science.215.4532.504.

Spencer, J. and Niebur, C. (2010) 'Mission Concept Study : Planetary Science Decadal Survey Enceladus Orbiter'. Pasadena, California: Jet Propulsion Laboratory, NASA.

Ultimaker (2018) 'Technical Data Sheet: Polycarbonate'. Ultimaker, pp. 1–3. Available at: https://ultimaker.com/download/74975/UM180821 TDS PC RB V11.pdf.

Ultimaker (2019a) 'Ultimaker 3: Specification sheet'.

Ultimaker (2019b) *Ultimaker 3*. Available at: https://ultimaker.com/en/products/ultimaker-3 (Accessed: 13 June 2019).

Vilán Vilán, J. A., Agelet, F. A., Estévez, M. L. and Muiño, A. G. (2015) ‘Flight results: Reliability and lifetime of the polymeric 3D-printed antenna deployment mechanism installed on Xatcobeo & Humsat-D’, *Acta Astronautica*, 107, pp. 290–300. doi: 10.1016/j.actaastro.2014.10.015.

Watanabe, S., Tsuda, Y., Yoshikawa, M., Tanaka, S., Saiki, T. and Nakazawa, S. (2017) ‘Hayabusa2 Mission Overview’, *Space Science Reviews*. Springer Science+Business Media Dordrecht, 208(1–4), pp. 3–16. doi: 10.1007/s11214-017-0377-1.

Wohlers Associates Inc. (2017) *Wohlers Report 2017*. Fort Collins, Colorado.

APPENDIX I

Measurements and inspection sheet of test specimen, pre- and post-treatment.

[1] = STRAIGHT OUT OF PRODUCTION, NO TREATMENTS

[2] = POST TREATMENT

All measurements in millimeters [mm]

Type	Specimen ID	Material	Color [1]	Defects [1]	t [1]	m1 [1]	m2 [1]	m3 [1]	m4 [1]	Comments [1]	Color [2]	Defects [2]	t [2]	m1 [2]	m2 [2]	m3 [2]	m4 [2]	Comments [2]
AM	A1	PC	WHITE	None	3,9	20,7	10,7	20,7	150,1	Even thickness , no warp	No change	None	4,1	20,7	10,8	20,8	146,2	Shortening in length
AM	A2	PC	WHITE	None	3,9	20,5	10,6	20,5	150	Even thickness , no warp	No change	None	4,1	20,4	10,6	20,6	145,5	Shortening in length
AM	A3	PC	WHITE	None	3,9	20,7	10,6	20,6	150	Even thickness , no warp	No change	None	4,1	20,6	10,7	20,7	145,8	Shortening in length
AM	A4	PC	WHITE	None	3,9	20,65	10,8	20,7	150,5	Even thickness , no warp, some black contaminant	No change	None	4,1	20,6	10,7	20,4	146,3	Shortening in length
AM	A5	PC	WHITE	None	3,85	20,8	10,8	20,6	150,7	Even thickness , no warp	No change	None	4,1	20,8	10,7	20,8	146,6	Shortening in length
AM	A11	PVDF-C	NATURAL	See comment	3,7	20,2	10,1	20,2	148,9	Even thickness , no warp, saw tooth top layer edge	No change	None	3,9	20,2	10,2	20,2	148,2	
AM	P1	PC	WHITE	None	3,8	20,6	10,7	10,7	150,7	Even thickness , no warp	-	-	-	-	-	-	-	-
AM	B1	PC	WHITE	None	3,9	20,7	10,7	20,8	150,5	Even thickness , no warp, some black contaminant	-	-	-	-	-	-	-	-
AM	B2	PC	WHITE	None	3,9	20,6	10,7	20,7	150,5	Even thickness , no warp	-	-	-	-	-	-	-	-
AM	B3	PC	WHITE	None	3,8	20,7	10,8	20,8	150,7	Even thickness , no warp	-	-	-	-	-	-	-	-
AM	B4	PC	WHITE	None	3,9	20,8	10,7	20,6	150,5	Even thickness , no warp	-	-	-	-	-	-	-	-
AM	B5	PC	WHITE	None	3,9	20,7	10,8	20,8	150,4	Even thickness , no warp	-	-	-	-	-	-	-	-